Techniques to Improve the Characterization of Protein Particles in Biologic Drug Products

By

Maria Toler

Submitted to the graduate degree program in Pharmaceutical Chemistry and the Graduate Faculty of the University of Kansas in partial fulfillment of the requirements of the degree of Master of Science.

_____
Chairperson Jennifer S. Laurence, Ph.D.

_____
David B. Volkin, Ph.D.

_____
Satish Singh, Ph.D.

_____
Susan Martin, Ph.D.

Date Defended: March 6, 2012

The Dissertation Committee for Maria Toler certifies that this is the approved version of the following dissertation:

Techniques to Improve the Characterization of Protein Particles in Biologic Drug Products

_____

Chairperson Jennifer S. Laurence, Ph.D.

Date Approved: May 7, 2012

Abstract

The characterization of particulate matter, especially protein aggregates, in the sub-visible and visible size range has become an area of focus in the biopharmaceutical industry. This heightened focus is due, in part, to increasing concern around particles causing immunogenicity, and increased queries from regulatory bodies. There has been extensive research in this area, with many recent publications on related methodologies, mechanisms and influencing factors. Two areas of interest are the characterization of these particles using material sparing approaches and the effect of the presence of silicone oil particles on protein solutions.

With the focus on high concentration drug products (≥50 mg/mL), and the drive toward conserving drug product by producing fewer batches, there is a real need for characterization techniques that require less sample. In addition, there is significant interest by the regulatory agencies in obtaining information on particulate matter in biologic drug products over a broad range of sizes. Queries are being generated by the FDA and other regulatory bodies, asking for particle count and any additional compositional information. They are requiring the pharmaceutical industry to have a deeper understanding of the formation of protein particles as well as methods for monitoring a broad range of sizes, over the shelf life of the product.

The propensity exists for increased protein aggregation at higher concentrations, yet companies are generating less sample material for testing during development. The focus

of this dissertation was to develop approaches for characterizing protein aggregation (particulates) using minimal sample amounts. To develop validatable methods for ongoing drug product monitoring as well as more novel approaches to better understand the nature of particulate matter present in biologic drug products. Silicone oil is present in many drug product contact surfaces and was chosen for further study on the effect of protein aggregation. The methods developed during this research were utilized to characterize protein and/or silicone oil particles, and to provide differentiation between protein and non-protein particles.

Acknowledgements

I would like to thank Jennifer Laurence, my mentor, whose patience has been most appreciated. Being a distance student and employed full time, it can be difficult to balance the requirements for all areas, but Dr. Laurence has proven to be a very caring and understanding mentor. In addition, my industrial mentor Susan Martin has been extremely helpful, and I appreciate her ability to keep me focused on what I needed to do to complete this research. I have worked closely with Satish Singh and appreciate his insight and continued guidance and thank him for serving on my defense committee. Lastly, I would also like to thank Dr. David Volkin for taking the time to review my work and sit on my defense committee.

TABLE OF CONTENTS

Chapter 1. Issues with Particles in Biologic Samples

1.1 Introduction

The number of biopharmaceutical products being submitted for FDA approval has rapidly increased over the last several years. In 2009, the FDA granted 18 full approvals for biopharmaceutical products [1]. This was the highest number of new product approvals since 2005. Proteins used in these biologics can be susceptible to self-association which can lead to aggregation. This is especially true for products being formulated at higher concentrations (usually >50 mg/mL). These aggregates can range in size from a few monomer units to hundreds of microns.

Protein aggregation has been an area of study for many years. Aggregates form as a result of association of protein molecules. This occurs from some instability of the protein in its environment. These instabilities have been well studied and can be caused by chemical and/or physical means [2, 3]. A protein aggregate has been described as a species of higher molecular weight (a multimer) that can be associated by covalent bonds or non-covalent interactions [4]. Non-covalent aggregates are formed by weak forces such as Van der Waals interactions, hydrogen bonding, hydrophobic and electrostatic interactions. Covalent aggregates can be formed from disulfide linkages through free thiol groups or non-disulfide cross linking pathways such as dityrosine formation. Self association of proteins can occur with changes in formulation parameters such as pH, ionic strength, buffer species or from high protein concentration (macromolecular

crowding). Aggregation can also be affected by temperature, mechanical stress (shaking, pumping, stirring) and interactions with foreign particles from contact surfaces (causing nucleation).

There are several models for protein aggregate formation, including:

1. Lumry-Eyring two state model, where

   Native protein→ reversible conformational change (aggregation prone state)→ assembly to an irreversible aggregated state.

2. Nucleation-propagation polymerization mechanism, where the nucleus can be from altered monomer or multimer species.

3. Heterogeneous nucleation, where aggregation is induced by micro/nanoparticles of foreign matter.

There are two main types of protein instabilities, chemical and physical. Chemical instabilities can lead to new chemical entities, whereas physical instabilities do not cause a change in chemical composition.

<u>Chemical instability</u>

Deamidation is considered one of the most common chemical degradation pathways, involving the hydrolysis of Asn and Gln side chain amides. In peptides, the main factors that affect deamidation rates are the protein primary sequence, temperature and pH [5, 6]. In folded proteins, the secondary and tertiary structure influences the rate of deamidation,

most often slowing the degradation process but in some cases accelerating the reaction [7, 8]. Hydrolysis can occur at the peptide backbone. Asp hydrolysis (also known as proteolysis), involves intramolecular cyclization and the rate is pH dependent and can be caused by buffer catalysis. Hydrolysis can occur, even when Asp is not present. Some IgG1's have been shown to undergo hydrolysis in the hinge region [9]. For some mAbs, this reaction can be metal catalyzed. There are other chemical reactions that can occur with proteins such as racemization, B-elimination, pGlu formation, and glycation (a Maillard reaction). Another primary chemical degradation pathway is oxidation, which can affect any protein containing His, Met, Cys, Tyr, and Trp amino acids. These amino acids can react with reactive oxygen species (free radicals that can be generated from a variety of sources) at any time during the development of a protein drug product. The reaction is nearly pH independent. A common residue to track for potential oxidation is Met. It is very sensitive to oxidation, even in the presence of molecular oxygen (as long as the residue is accessible by the solvent it is present in). Other oxidation reactions include metal-catalyzed oxidation, Trp oxidation, photo-oxidation, and cysteine oxidation. Photolytic degradation can occur from light exposure leading to photo-oxidation of side chains of amino acids such as Met, Tyr, Trp, His, Cys, and Phe and has been shown to induce protein aggregation [4].

Physical instability

Denaturation is a common term for physical degradation of a protein, which involves a change in the three dimensional structure (such as unfolding). Denaturation, however, can involve changes to the secondary or tertiary structure. Thermal denaturation is a

common mechanism of instability, usually caused by exposing the protein to elevated temperatures causing partial or full unfolding. The unfolded molecules will tend to associate forming aggregates. Other forms of denaturation include cold denaturation, chemical and pressure-induced denaturation. Denaturation can also occur with exposure to a mechanical stress as described earlier.

All of the instabilities reviewed (both chemical and physical) can lead to protein states that are amenable to aggregation. An aggregate involves the association of protein molecules, which can come from covalent or non-covalent interactions, and vary greatly in the degree of reversibility. Small aggregates are often soluble. As these aggregates grow and continue associating, the resulting complexes can become large enough to detect visibly and often transform into insoluble particulates. These entities are considered non-reversible. One exception would be proteins that are salted-out, where the particles are insoluble, but retain activity and native-like structure. The formation of these particles is reversible upon dilution. The characterization of particulates is of great interest to the pharmaceutical industry and will be the topic of much of the research described in this dissertation.

Therapeutic protein aggregates have been linked to issues such as loss of efficacy and immunogenicity. Immunogenicity can be considered the ability of a material to induce an immune response in the body. This can occur with the first introduction of the drug or through repeated administration. For proteins that are human homologues (human-like), aggregation is the primary factor inducing immunogenicity [10]. It is this immunogenic

effect of protein products that is of great concern to the regulatory agencies and the pharmaceutical industry. A recent CMC Strategy Forum meeting was held to discuss analysis and immunogenic potential of protein aggregates and particles. Barry Cherney (DTP, CDER, FDA) was present and discussed arguments that have been made regarding the lack of direct evidence relating sub-visible protein aggregates to increased immunogenicity. Arguments include that fact that the amount of protein in these particles is too small to induce a response [11]. Cherney was clear in stating that the level required for a particular product to induce a response is not known, especially when repeated dosing is involved. The lack of data or knowledge does not eliminate the risk but creates unknown and uncontrolled risk. He stated that since there is no clear evidence that sub-visible particles are not critical, the type and amount of these particles should be considered a critical quality attribute (CQA) and must be monitored and controlled appropriately. It was clear from these discussions that measuring particulate matter during development and post approval is necessary and can be used to establish a direct link to clinical outcomes.

1.2 Sub-visible Particles

Compendial methods are in place to monitor sub-visible particle abundance in parenterals, such as the United States Pharmacopeia (USP<788>). The European and Japanese Pharmacopeia are harmonized with the USP. These methods utilize light obscuration as the method for detecting and counting sub-visible particles. These methods state that particle counts at 10 μm and greater and 25 μm and greater be monitored. As discussed previously, there is a need to detect smaller particles when

dealing with biologic products. The instruments can, depending on the sensor used, detect particles from approximately 1.5 to 400 μm. The methods do however, require a large sample volume for analysis (approximately 25 mL). The sample can be diluted if needed, but this is not ideal for protein solutions, where reversible aggregates can be affected.

An alternative to light obscuration particle counting in the compendia, is an optical microscopy technique where the test solution is filtered onto a membrane and particulates are counted. This technique is also optimized for detecting the presence of extrinsic or foreign particulate matter. It has many limitations when analyzing for protein particles, including lack of contrast between protein particles and the membrane surface as well as amorphous protein particles embedding into the filter and never being detected.

Another limitation to light obscuration is the lack of sensitivity to transparent particles. A technique based on micro-flow imaging (also known as flow microscopy) is gaining popularity as a means of counting sub-visible protein particles. Instruments such as the Brightwell Micro-flow Imaging system and the FlowCam are gaining popularity for characterization of biologic products. The technique is based on dynamic imaging of a sample as it flows past a high speed camera. Images are obtained and can be analyzed for particle concentration as well as morphological features. A study was performed by Glaxo Smith Kline comparing the ability of several techniques to detect protein aggregates versus a flow microscopy instrument [12]. Several protein formulations were subjected to freeze-thaw stress and monitored by flow microscopy, SEC (for % soluble

aggregate), icIEF (% main peak) and light obscuration. For each formulation, a control sample and stressed sample were compared. The only technique able to detect a difference in aggregate level was flow microscopy, where each formulation exhibited a 2-10 fold increase in sub-visible particles. Since micro-flow imaging was useful in detecting changes in aggregate levels, the team was able to look at the effect of excipients as stabilizers that prevent aggregate formation, such as Polysorbate 80. Micro-flow imaging does show promise as a technique for monitoring sub-visible particles in protein solutions, but limitations still exist with the technology.

The compendial methods were developed for monitoring the presence of extrinsic or foreign particulate matter in small molecule parenterals. These methods have some critical limitations when analyzing biologic drug products for the presence of sub-visible aggregates. Proteinaceous particles are amorphous, flexible and can vary greatly in morphology. They can be very close in refractive index to the matrix they are found in, making them virtually transparent. These optical and physical properties make them very challenging to detect using traditional sub-visible analysis approaches. In addition to the limitations due to the properties of protein particles, many times there is very little material available during the biologic drug development process. It is important to characterize the drug product throughout the development process. There have been studies showing that in some formulations, as the number of subvisible particles grow, larger aggregates form eventually leading to the formation of visible particulates in the product [11].

1.3 Visible Particles

Visible particles are usually described as particles >100 μm in size. At this size, the probability of detecting the particle is approximately 40%, and becomes greater than 95% for particles greater than or equal to 200 μm [13]. There are two primary methods for visible particle inspection- manual human inspection and automated inspection using a system such as the Eisai. These methods are excellent at detecting defects and foreign particulate matter but may not be as sensitive to transparent protein particles, especially under specified inspection conditions as described in USP Gen Chapter 1. Some of this limitation can be overcome with human inspection through proper training. There is also a concern that the motion used in automated inspection systems could induce aggregation in sensitive products. Some protein particles are very thin and transparent, creating a challenge for most inspection processes. As such, the use of dyes to enhance contrast may provide a solution to the detection of these types of particles.

In addition to detecting particles, it is becoming imperative that the composition be determined. Particle counts are a critical quality attribute, and identification of the particles is becoming a more frequently discussed issue. Cherney stated in the CMC forum meeting, techniques should be used to characterize the nature of particles detected [11]. This concept was further enforced in a recent publication by Wim Jiskoot et al. reviewing protein delivery systems. The paper stated that the industry is in urgent need of methods that are capable of discriminating between particles, whether they be protein related or matrix related [14]. The identification of particulate matter must be considered one of the necessary analytical methods used to monitor the physical stability of a

biologic. This dissertation provides modifications of current techniques and alternative methods to enhance detection and characterization of protein particles in the sub-visible and visible size range.

1.4 Silicone Oil

Although proteinaceous particles are an important topic for discussion, the presence of foreign particulates must be considered when characterizing biologic solutions. A very common extrinsic particle found in biologic drug products is silicone oil. Silicone oil is a common additive found in syringe barrels, certain stoppers, and inner surfaces of certain tubings and glass vials. In prefilled syringe devices, silicone oil is applied to the inner barrel to decrease the glide force, making self injections easier for the patient. Depending on the type of syringe, staked-in needle versus Luer lock, different processes of applying the silicone oil are used. For syringes with a Luer lock tip, the oil is sprayed on, rinsed and can be baked. Syringes with a staked in needle have the oil sprayed on, but due to the process of applying the needle, these syringes cannot be baked. In general, the process of baking the coating, helps it adhere and results in less oil leaching into the product. In many instances, the oil that has leached is emulsified and results in small spherical droplets in the drug product solution. There have been studies suggesting that silicone oil can induce protein aggregation, but many recent studies have demonstrated that silicone oil did not cause any aggregate formation [15, 16]. The stability of lyophilized Albinterferon Alfa-2b was monitored with and without silicone oil (post reconstitution) for 3 weeks at 25ºC [17]. Several levels of silicone oil were spiked into the samples. Over this time, silicone oil had no effect on the physical stability of the

material as determined by monitoring sub-visible particles by micro-flow imaging (the Brightwell). Protein secondary and tertiary structure was not affected, as determined by FTIR and CD spectroscopy. The authors noted that the formulation contained polysorbate 80, which may have protected the protein from silicone oil induced aggregation. This study demonstrates the type of characterization that should be performed when screening formulations for the effect of the presence of silicone oil. The authors state that greater than 98% of all particles were in the 1-10 μm size range. In addition, increased particle counts were observed with increased silicone oil levels. As mentioned previously, using the techniques outlined above, there was no easy way to determine if the increased counts were due to just neat silicone oil, or oil and protein interactions (such as protein coating the oil droplets). If the oil droplet morphology remained fairly equant, the analytical techniques used would not be able to detect any interaction with protein.

Another important factor to consider is the resolution of the images at small particle sizes (<10 μm). The resolution with current micro-flow imaging techniques is moderate. It is well known in the field of microscopy and image analysis that current imaging capabilities allow for resolution to approximately 5 μm. This limit also applies to micro-flow instruments, where the smallest object resolved is approximately 5 μm, and even more resolving power would be needed to perform any high level description of the particle [18]. Most particles will appear somewhat spherical at very small sizes, and it may be very difficult to distinguish a globular protein aggregate from an oil droplet, as shown in the gallery of images for a silicone oil sample and a sample of bovine serum

albumin (Figure 1.1). It is difficult to differentiate particle types until particles reach approximately 10 μm or greater.

Figure 1.1. The top set of images are silicone oil droplets, covering a range of particle sizes from 2-25 µm, obtained using a Brightwell MFI DPA4200. The bottom set of images are a BSA sample, covering the same size range of particles, 2-25 µm. Sizes are based on an equivalent circular diameter (ECD).

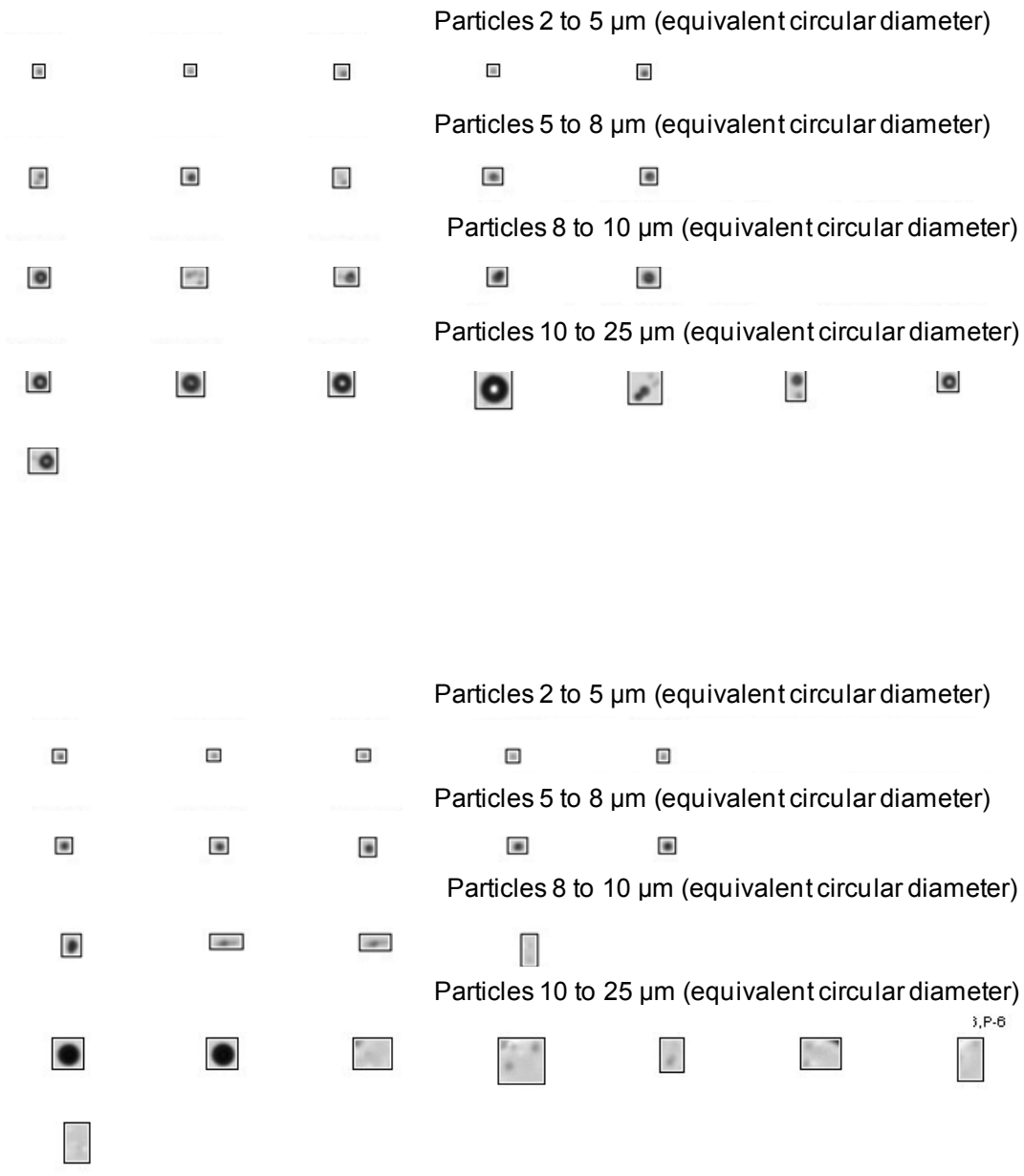

There have been several recent papers recommending the use of digital filters to remove particle counts when it is known that silicone oil is present in the sample. As shown above, with such poor resolution it is dangerous to exclude any particles from the total count. A recent study from Novartis showed application where it might be acceptable to digitally filter particles thought to be silicone oil [16]. A total of nine individual optical parameters were evaluated using images of solutions containing IgG-A and IgG-B protein particles along with silicone oil droplets. There was significant overlap between these values in the 2-15 μm size range. It was determined that no one parameter could provide adequate discrimination between protein particles and silicone oil droplets. This would lead to high levels of error in classifying the particles. Next, four optical parameters, along with cut-off values, were applied to analyze the same images. The optical parameters were circularity (how circular a particle is), aspect ratio (the ratio of length to width of a particle), object intensity STD (standard deviation in the intensity value for the particle image) and object intensity MAX (the maximum value for the particle image). This approach resulted in much better discrimination, especially above a particle size of approximately 5 μm. Another advantage to this approach is the ability to fine tune the optical parameters and cut-off values to accommodate protein particles with different optical properties. Although this approach does provide an interesting solution to discriminating silicone oil droplets, thus allowing for digitally excluding them, some knowledge of the particles present in solution must be obtained initially. Also, this approach cannot determine if the silicone oil particles are associated with protein,

especially if the overall morphology remains fairly spherical. This is important because even non-protein particles coated in protein can be highly immunogenic [11].

1.5 Outline of the Dissertation

This dissertation provides approaches to aid in the characterization of sub-visible and visible protein particles, using a minimal amount of test material. As discussed in the introduction, pharmaceutical companies are being asked to provide more detailed information on the abundance and type of particles present in biologic drug products. Chapter 2 provides details on the development and qualification of a procedure for using light obscuration, as described in USP <788>, but with much less sample volume, and the ability to monitor particles down to 2 μm in size. In addition, the Brightwell micro-flow imaging system was compared to the light obscuration technique, focusing on possible causes for the discrepancy in particle counts consistently obtained when comparing these techniques. Chapter 3 describes the use of a visible protein specific dye to be used in conjunction with optical microscopy. As discussed previously, protein aggregates can be very difficult to detect by optical microscopy, even with optimized lighting conditions. Also, protein particles can be difficult to impossible to detect when filtered onto a membrane for characterization. A dye can enhance the contrast between a protein particle and its matrix or a filter membrane. This allows for visualization by microscopy as well as the ability to apply image analysis techniques to obtain both qualitative and quantitative information about the aggregates. With the use of microscopy, both visible and sub-visible particles can be detected, down to approximately 1-2 μm. Lastly, Chapter 4 describes an investigation of silicone oil droplets in the presence of protein

solutions/aggregates. The possibility of protein coating silicone oil particles was probed. By using a fluorescent dye, silicone oil droplets associated with protein were detectable. This work could prove useful as a technique for understanding when silicone oil droplets can or cannot be ignored.

Chapter 2. Particle Size and Count Methods

2.1 Development and Validation of a Low Volume Light Obscuration Method, with Detection Below 10 µm

2.1.1 Introduction

Light obscuration testing for the quantitation of sub-visible particle counts is an established technique and cited in the compendia (eg; USP, EP, JP). These compendia are harmonized on the testing procedures; therefore USP<788> was cited when referring to compendial requirements. The compendial method requires a large amount of test solution per sample analyzed (approximately 25 mL for a single analysis) [19]. During the development of a biologic, it would be of great benefit to monitor sub-visible particle counts but the amounts of solution required per the USP would be prohibitive. It was desired to develop a method that would provide sub-visible particle count results using significantly less test volume.

In addition to minimizing sample requirements, it was desired to monitor the particle counts below the compendial limit of 10 µm. There is much discussion around the need to begin monitoring particle counts less than 10 µm. In very recent years, the FDA has been asking pharmaceutical companies to provide additional particle count information for particles 1-2 µm and greater, in part due to the increased publications discussing the role of sub-10 µm protein particles in inducing immunogenicity [20].

The HIAC light obscuration instrument is commonly used for USP<788> testing. This type of method development is occurring within the pharmaceutical industry and will aid in our understanding of protein particle formation [21].This instrument can be modified to monitor particles down to approximately 2 μm. It can also be equipped with a smaller gauge aspirator, allowing for lower volumes to be tested. A study was performed to develop a HIAC method that would require minimal sample volume while analyzing particles in the 1.5-10 μm range as well as the 10-150 μm size range.

2.1.2 Materials and Methods

For this study, a HIAC/Royco Pacific Scientific Liquid Particle Counting System (model 9703) was used for all light obscuration results. A 10 mL aspirator was used with the instrument to allow for reduced test volumes. A HRLD 150 sensor was installed in the instrument. This sensor has a lower limit of detection of approximately 1 μm and an upper limit of 150 μm, allowing for monitoring particle counts down to 1.5 um. A flow rate of 25 mL/min was used for all studies. Particle count data were acquired using PharmSpec 2.0 software.

Samples were handled under clean conditions, in a lab containing HEPA filtered air. All test solutions were handled in a laminar air flow hood. The conditions for testing meet suggested environmental conditions as described in USP<788>. In addition, any glassware used during the study was pre-rinsed using particle free water, and stored in the laminar flow hood. Any sample dilution, as well as instrument rinsing was performed

using MilliQ water (0.2 µm filtered). A set of latex microsphere standards (NIST traceable) were used for this work, as describe in Table 2.1. These standards contained monomodal size distributions at the nominal sizes stated. In addition, bovine serum albumin (Sigma #A4503) was used in a robustness study.

Table 2.1. Latex particle standard information

Item	Vendor	Catalog #
Particle Count Standard- 2 um	Thermo Fisher	CC2-PK
Particle Count Standard- 15 um	Thermo Fisher	CC15-PK
Particle standard-5 um	Thermo Fisher	9005
Particle standard-15 um	Thermo Fisher	9015

2.1.2.1 Experimental Design

The HIAC instrument used was calibrated by the vendor, on a 6 month schedule. The calibration was extended over the complete size range, from 1 µm to 100 µm. In addition, flow rate and aspiration volume accuracy were also qualified by the vendor before any experimentation. A daily system suitability test was also performed, ensuring that the instrument particle counts met the certified value for the 15 µm particle standard.

2.1.2.2 Test Parameters

Accuracy

Count accuracy was determined using 15 µm and 2 µm certified count standards, neat. Both 0.5 mL and 1 mL injections were evaluated. Four injections and six injections were evaluated per test volume, with the first injection discarded in all cases. This is necessary since the first injection can have aberrant count values due to mixing of sample and rinse solution in the instrument. The average cumulative counts per sample were recorded, and compared to the certified values available from the vendor.

Linearity

For this study, the 2 µm, 5 µm and 15 µm count standards were used. A series of dilutions were created as shown in Table 2.2. Each dilution was evaluated at a set of injection volumes including 0.5 mL, 1 mL, and 5 mL (5 mL being the volume described in USP<788>, and used for comparison to lower volumes tested). The average cumulative counts per sample were recorded. For the 2 µm standard, the cumulative counts at 1.5 µm were used. For the 5 µm standard, the cumulative counts at the 2.5 µm size were used. For the 15 µm standard, the cumulative counts at 10 µm were used. It was critical that the counts at a size bin below the nominal standard size was used, since the particles comprise a normal distribution around the nominal particle size and all particles contributing to that distribution must be accounted for.

Table 2.2. Dilution scheme for linearity test sample preparation.

	Dilution 1	Dilution 2	Dilution 3	Dilution 4	Dilution 5
Dilution conc (p/mL)	1000	500	200	100	25
Standard (mL)	25 mL stock	35 mL D1	30 mL D2	35 mL D3	10 mL D4
Water (mL)	50	35	45	35	30
Total vol (mL)	75	70	75	70	40

Precision

The precision of a measurement is a critical parameter to evaluate. Knowing the precision of a measurement aids in determining if two results are truly different. Two vials of a standard particle suspension (22 mL each) were combined. To this, 88 mL water was added for a total volume of 132 mL at 1000 particles/mL. The suspension was analyzed at 5 mL, 1 mL and 0.5 mL injection volumes over 3 days (again, the first injection will be discarded for all runs). A second sample was analyzed, diluted to the lower limit of detection to determine precision at low particle concentration. The study design is shown in Table 2.3. All conditions were compared to the variability obtained with the 5 mL injection volume since this is the compendial method parameter.

Table 2.3. Design of study to determine the precision of the particle count measurements.

Injection Volume (mL)	No. Injections	No. Replicates	No. Days	Total Volume (mL)
5	4	1	3	60
1	4	3	3	36
0.5	4	3	3	18

Specificity

A study was conducted to look at the specificity of the particle count value when two particle size standards with significantly different concentrations were present in a single sample. Two mixtures were created as shown in Table 2.4. Both 5 mL and 1 mL injection volumes were evaluated versus expected concentration values.

Table 2.4. Two stock solutions were prepared to evaluate the specificity of the particle count measurement.

Stock #1

Standard	Standard vol. (mL)	No. Particles	Final conc. after adding 50 mL water
2 µm	5	15,000	200 (particles/mL)
15 µm	20	60,000	800 (particles/mL)

Stock #2

Standard	Standard vol. (mL)	No. Particles	Final conc. after adding 50 mL water
15 µm	5	15,000	200 (particles/mL)
2 µm	20	60,000	800 (particles/mL)

Robustness Studies

Samples were tested for appropriate time and mode of degassing. Samples were degassed by allowing to sit at ambient conditions for a specified period of time (0, 2, 5, 10, 15, 20 and 30 minutes), or sonicated using a sonic bath for 30 or 60 seconds (additional time could be too aggressive for protein solutions, and could cause aggregation). A last method of degassing was to place the sample under vacuum in a bell jar. Samples were tested after 30 seconds, 2, 10, 20 and 30 minutes under vacuum.

Samples included 2 platform formulation buffers (Form A and Form B), particle free water and Form B with 10 mg/mL BSA added. Form A buffer contained 10 mM potassium phosphate, pH 7.4 and Form B buffer contained 10 mM histidine, pH 6.0. Samples were mixed by vigorous manual shaking (inverting the vials) 30 times.

2.1.3 Results

2.1.3.1 Accuracy

The count accuracy was tested using two standards, with different nominal diameters. All standards had a certified particle concentration of 3000 particles/mL ± 10%. This concentration was used as the acceptance criteria for the samples. Each sample was tested using either 4 or 6 total injections (with the first injection discarded from the results when averaged). The results are shown in Table 2.5. The 0.5 mL injection volume failed the acceptance criteria for each sample with the counts always being biased low at this injection volume. It was determined that 4 injections (with the first injection discarded and not included in the averaging of the results), using 1 mL volume, were accurate for particle count. The 1 mL injection volume resulted in low percent relative standard deviations (%RSD) for all samples tested.

Table 2.5. Particle count results for the accuracy study using 2 and 15 µm.

Stnd	# Injections	Inj vol (mL)	Mean Particles/mL	Standard Deviation	%RSD	Acceptance criteria (particles/mL)
2 µm	4	0.5	2561	79	3	2700-3300
2 µm	4	1	2791	32	1	2700-3300
2 µm	6	0.5	2644	92	3	2700-3300
2 µm	6	1	2781	20	1	2700-3300
15 µm	4	0.5	2537	31	1	2700-3300
15 µm	4	1	2904	45	2	2700-3300
15 µm	6	0.5	2591	40	2	2700-3300
15 µm	6	1	2808	15	1	2700-3300

2.1.3.2 Linearity

The linearity associated with particle counts was evaluated by analyzing a series of particle concentrations, covering a range of particle size. It was determined in the accuracy study that a 0.5 mL injection volume would not produce a count within the acceptable range. Based on this information, 1 mL and 5 mL (USP suggested volume) injection volumes were evaluated. A total of 4 injections were used (with the first injection result discarded). A series of 5 dilutions were made using 2, 5 and 15 µm count standards as described previously in this report. The tested particle dilutions ranged from 1000 particles/mL to 25 particles/mL. Tables 2.6 to 2.8 show the particle count results for each particle size standard tested. The data tables include the standard deviation and percent relative standard deviation (%RSD) for the three injections. In addition, the % difference from the resulting concentration versus the target concentration is calculated for each dilution level. The % difference was always higher at the highest dilution (Dilution #5) because the concentrations were very low at this level. Low counts such as this are approaching the noise of the system and are highly variable.

Table 2.6. Results for the linearity test with the 2 μm standard (N=3).

Stnd	Dil#	Inj Vol (mL)	Resulting Conc (particles/mL)	Standard Deviation	%RSD	Target Conc (particles/mL)	%Diff
2	1	1	1064	45.79	4.302	1000	6
2	2	1	564	18.6	3.30	500	13
2	3	1	210	14.6	6.93	200	5
2	4	1	102	8.50	8.37	100	2
2	5	1	33	3.0	9.1	25	32
2	1	5	1013	5.100	0.4625	1000	1
2	2	5	599	9.34	1.56	500	20
2	3	5	224	5.77	2.58	200	12
2	4	5	114	3.70	3.25	100	14
2	5	5	33	1.9	5.7	25	31

Table 2.7. Results for the linearity test with the 5 μm standard (N=3).

Stnd	Dil#	Inj Vol (mL)	Resulting Conc (particles/mL)	Standard Deviation	%RSD	Target Conc (particles/mL)	%Diff
5	1	1	958	11.9	1.25	1000	-4
5	2	1	470	21.0	4.47	500	-6
5	3	1	193	17.2	8.90	200	-4
5	4	1	103	18.6	18.0	100	3
5	5	1	30	8.0	27	25	20
5	1	5	1001	10.51	1.049	1000	0
5	2	5	516	4.70	0.911	500	3
5	3	5	206	8.16	3.96	200	3
5	4	5	109	5.51	5.03	100	9
5	5	5	29	2.1	7.3	25	16

Table 2.8. Results for the linearity test with the 15 µm standard (N=3).

Stnd	Dil#	Inj Vol (mL)	Resulting Conc (particles/mL)	Standard Deviation	%RSD	Target Conc (particles/mL)	%Diff
15	1	1	969	11.4	1.17	1000	-3
15	2	1	481	12.5	2.60	500	-4
15	3	1	202	8.74	4.33	200	1
15	4	1	102	7.23	7.07	100	2
15	5	1	31	7.5	24	25	24
15	1	5	1002	8.900	0.8881	1000	0
15	2	5	487	4.69	0.962	500	-3
15	3	5	205	15.1	7.37	200	3
15	4	5	104	6.20	5.95	100	4
15	5	5	33	0.70	2.1	25	33

The data was also plotted, overlaying the resulting concentrations obtained for both injection volumes per sample dilution tested. Figures 2.1 to 2.3 demonstrate that the same results were obtained regardless of the injection volume. All samples, regardless of injection volume resulted in linear curves over the particle concentration tested. The lines overlay perfectly, with very small error bars and good fit for each line (R^2 values of at least 0.999), as shown in the plots. The 1 mL injection was shown to be equivalent to the 5 ml injection volume under the test conditions used, which indicates that using a 1 mL injection would provide particle counts in compliance with USP<788>. The

concentration range tested is broad as would be expected when testing a variety of solutions, where very low counts might be encountered for a blank or very dilute protein solution and the higher counts (1000 particles/mL) are common for higher concentration protein solutions or stressed samples.

Figure 2.1. Plot of particle counts for 1 mL and 5 mL injection volumes, over a range of concentrations (dilutions) for the 2 µm standard. Error bars represent ± 1 standard deviation (N=3).

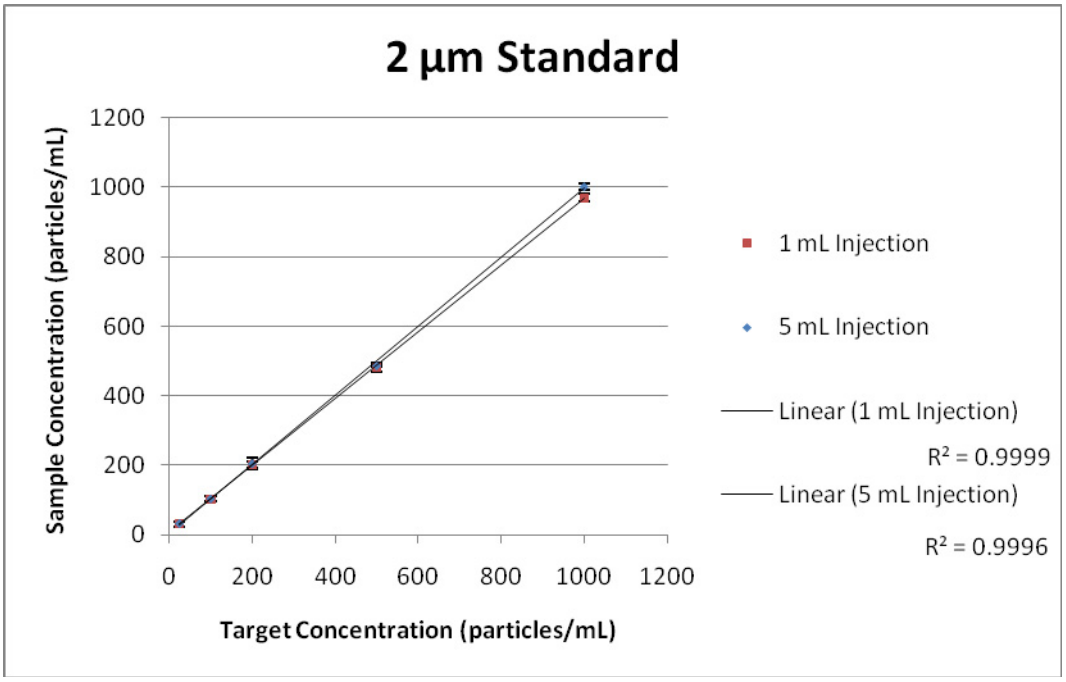

Figure 2.2. Plot of particle counts for 1 mL and 5 mL injection volumes, over a range of concentrations (dilutions) for the 5 µm standard. Error bars represent ± 1 standard deviation (N=3).

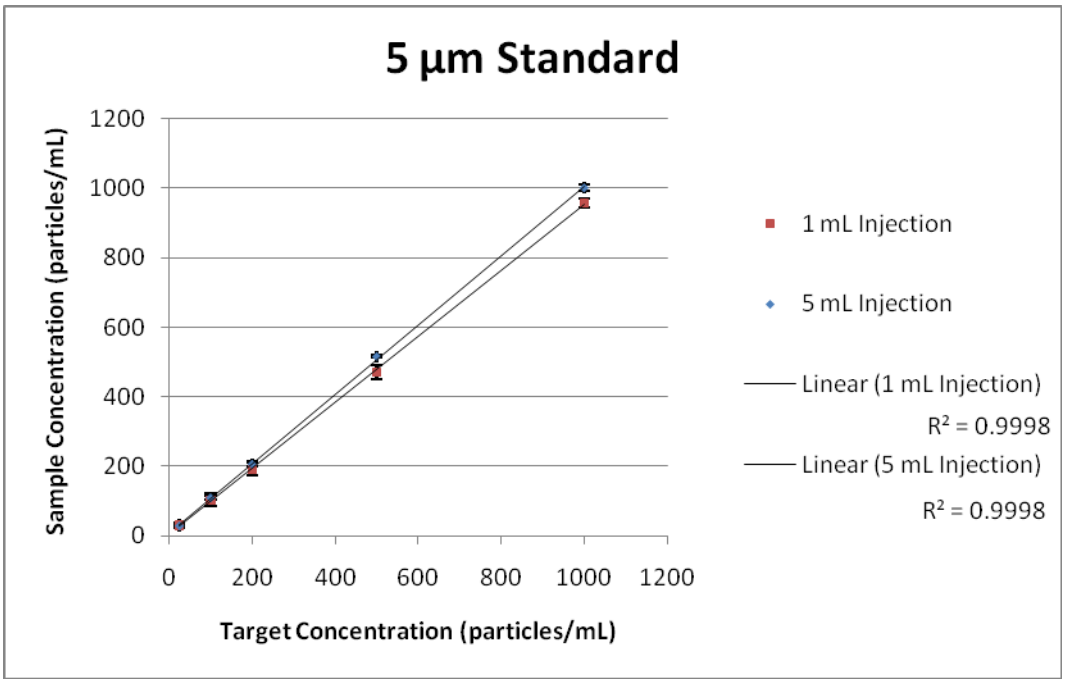

Figure 2.3. Plot of particle counts for 1 mL and 5 mL injection volumes, over a range of concentrations (dilutions) for the 15 µm standard. Error bars represent ± 1 standard deviation (N=3).

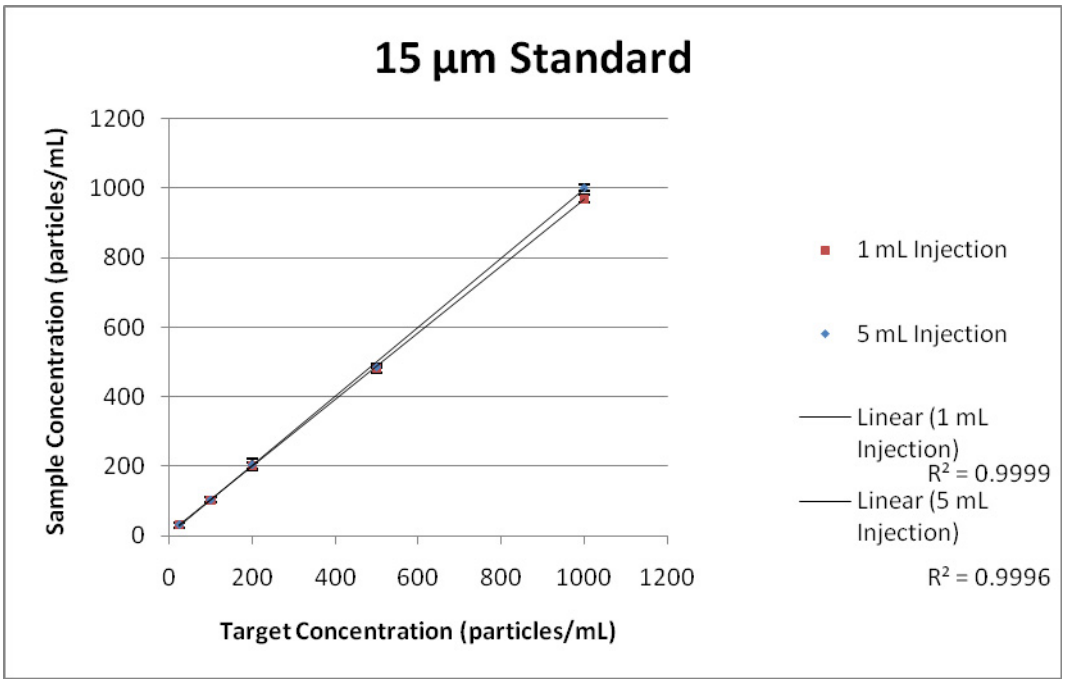

2.1.3.3 Precision

Precision measurements were made for the 0.5 mL injection volume using a limited number of samples because the accuracy was less than desired. The 1 mL injection volume, found to be the most suitable test volume, was analyzed for repeatability and reproducibility of the measurement. In addition a set of injections at 5 mL (compendial volume) was performed for comparison using a limited data set. The average cumulative counts (particles/mL) for 3 injections (4 injections were made, with the first being discarded) is shown in the summary table (Table 2.9). The repeatability of the

measurement (average of runs performed on a single day), and the reproducibility of the measurement (average of runs over 3 days testing) were calculated. The cumulative counts for the appropriate size range were evaluated, where cumulative counts at 1.5 µm encompass the results for the 2 µm standard and cumulative counts at 10 µm encompass the results for the 15 µm standard. The measurement error was captured in this testing, whereas the procedural error was not accounted for due to the nature of the sample preparation. Table 2.10 is a summary of the average counts (particles/mL) for all injections per sample, averaged over all days of testing. For all results, the standard deviation (SD) and percent relative standard deviation (%RSD) were calculated.

Table 2.9. Particle count results for each sample tested. The statistics for the reproducibility and repeatability are shown.

								N=3 runs, repeatability (same day)			N=3 runs, reproducibility (3 days)		
Sample Name	**Standard Size (µm)**	**Stnd Conc p/mL**	**Inj Vol (mL)**	**Run#**	**Day**	**Avg Cum p/mL 2 µm**	**Avg Cum p/mL 15 µm**	**AVG**	**SD**	**%RSD**	**AVG**	**SD**	**%RSD**
2 um 25 p/mL	2	25	0.5	1	1	35.33	0.67						
	2	25	0.5	2	1	42.67	8.67						
	2	25	0.5	3	1	30	0	36	6.4	17.7			
	2	25	0.5	1	2	34.67	0						
	2	25	0.5	2	2	23.33	0						
	2	25	0.5	3	2	34	1.33	31	6.4	20.7			
	2	25	0.5	1	3	42.67	6.67				38	4.4	11.8
	2	25	1	1	1	33.33	0						
	2	25	1	2	1	35.67	0.33						
	2	25	1	3	1	37.67	0.33	36	2.2	6.1			
	2	25	1	1	2	27.67	0						
	2	25	1	2	2	36	0						
	2	25	1	3	2	40	0.33	35	6.3	18.2			
	2	25	1	1	3	38.33	0						
	2	25	1	2	3	42	0						
	2	25	1	3	3	33.67	0.33	38	4.2	11.0	33	5.3	16.1
	2	25	5	1	1	36.07	0.47						
	2	25	5		2	38.67	0.13						
	2	25	5		3	36.13	0.27				37	1.5	4.0

Table 2.9 continued.

								N=3 runs, repeatability (same day)			N=3 runs, reproducibility (3 days)		
Sample Name	**Standard Size (µm)**	**Stnd Conc p/mL**	**Inj Vol (mL)**	**Run#**	**Day**	**Avg Cum p/mL 2 µm**	**Avg Cum p/mL 15 µm**	**AVG**	**SD**	**%RSD**	**AVG**	**SD**	**%RSD**
2 um 1000 p/mL	2	1000	0.5	1	1	880	0						
	2	1000	0.5	2	1	872	7.33						
	2	1000	0.5	3	1	883.33	4	878	5.8	0.7			
	2	1000	0.5	1	2	870	0.67						
	2	1000	0.5	1	3	867.33	0.67				872	6.7	0.8
	2	1000	1	1	1	976.67	0.67						
	2	1000	1	2	1	947.33	1.33						
	2	1000	1	3	1	935.33	2.33	953	21.3	2.2			
	2	1000	1	1	2	946	1						
	2	1000	1	2	2	960.67	1						
	2	1000	1	3	2	976.67	1	961	15.3	1.6			
	2	1000	1	1	3	950.33	2						
	2	1000	1	2	3	1091.67	10						
	2	1000	1	3	3	985.67	0.67	1009	73.6	7.3	958	16.6	1.7
	2	1000	5	?	1	1007.47	0.87						
	2	1000	5		2	1003.93	1						
	2	1000	5		3	1015.73	1.07				1009	6.1	0.6

Table 2.9 continued.

								N=3 runs, repeatability (same day)			N=3 runs, reproducibility (3 days)		
Sample Name	**Standard Size (µm)**	**Stnd Conc p/mL**	**Inj Vol (mL)**	**Run#**	**Day**	**Avg Cum p/mL 2 µm**	**Avg Cum p/mL 15 µm**	**AVG**	**SD**	**%RSD**	**AVG**	**SD**	**%RSD**
15 um 25 p/mL	15	25	0.5	1	1	44	30						
	15	25	0.5	2	1	44.67	25.33						
	15	25	0.5	3	1	32.67	20.67	25	4.7	18.4			
	15	25	0.5	1	2	47.33	24.67						
	15	25	0.5	2	2	44.67	24.67						
	15	25	0.5	3	2	41.33	24.67	25	0.0	0.0			
	15	25	0.5	1	3	34	17.33				24	6.4	26.5
	15	25	1	1	1	37	23.33						
	15	25	1	2	1	43.33	29						
	15	25	1	3	1	48.67	30.67	28	3.8	13.9			
	15	25	1	1	2	42.33	24.33						
	15	25	1	2	2	51	26.33						
	15	25	1	3	2	44	26.67	26	1.3	4.9			
	15	25	1	1	3	44	23.67						
	15	25	1	2	3	40.67	26						
	15	25	1	3	3	37.67	22.33	24	1.9	7.7	24	0.5	2.1
	15	25	5		1	41.67	25.27						
	15	25	5		2	43.2	26.6						
	15	25	5		3	44.07	23.13				25	1.8	7.0

Table 2.9 continued.

								N=3 runs, repeatability (same day)			N=3 runs, reproducibility (3 days)		
Sample Name	**Standard Size (µm)**	**Stnd Conc p/mL**	**Inj Vol (mL)**	**Run#**	**Day**	**Avg Cum p/mL 2 µm**	**Avg Cum p/mL 15 µm**	**AVG**	**SD**	**%RSD**	**AVG**	**SD**	**%RSD**
15 um 1000 p/mL	15	1000	0.5	1	1	919.33	901.33						
	15	1000	0.5	2	1	889.33	867.33						
	15	1000	0.5	3	1	918.67	892.67	887	17.7	2.0			
	15	1000	0.5	1	2	906	884.67						
	15	1000	0.5	2	2	905.33	879.33						
	15	1000	0.5	3	2	912	886	883	3.5	0.4			
	15	1000	0.5	1	3	874.67	841.33				876	31.0	3.5
	15	1000	1	1	1	933.67	908.67						
	15	1000	1	2	1	940	913.67						
	15	1000	1	3	1	951	926.33	916	9.1	1.0			
	15	1000	1	1	2	925	900.33						
	15	1000	1	2	2	993.67	964.67						
	15	1000	1	3	2	978.33	954.67	940	34.6	3.7			
	15	1000	1	1	3	959.33	931.67						
	15	1000	1	2	3	886.67	859.67						
	15	1000	1	3	3	831.67	807.67	866	62.3	7.2	914	16.2	1.8
	15	1000	5		1	1009.8	984.53						
	15	1000	5		2	1024.2	996.67						
	15	1000	5		3	1013.33	983.27				988	7.4	0.7

Table 2.10. Particle count results for each sample, averaged over all days runs. The standard deviation (SD) and percent relative standard deviation (%RSD) are reported.

Sample Name	Injection volume (mL)	No. of Runs	Avg particles/mL	SD	%RSD
2 um, 25 p/mL	0.5	7	35	6.8	20
2 um, 25 p/mL	1	9	36	4.2	12
2 um, 25 p/mL	5	3	37	1.5	4.0
2 um, 1000 p/mL	0.5	5	875	6.82	0.780
2 um, 1000 p/mL	1	9	974	47.1	4.83
2 um, 1000 p/mL	5	3	1009	6.055	0.6001
15 um, 25 p/mL	0.5	7	24	4.0	17
15 um, 25 p/mL	1	9	26	2.7	11
15 um, 25 p/mL	5	3	25	1.8	7.0
15 um, 1000 p/mL	0.5	7	879	19.7	2.24
15 um, 1000 p/mL	1	9	907	48.4	5.34
15 um, 1000 p/mL	5	5	988	7.40	0.749

2.1.3.4 Specificity

Mixtures of 2 and 15 μm particles were created (Stock 1 and 2) to determine the specificity of particle counting in a mixed sample. The results showed that the larger particle size was greatly undercounted in the presence of the smaller particles, regardless of the ratio in counts between particle sizes (Table 2.11). In addition, the injection volume did not affect the results. This undercounting was unexpected and suggests that some optical condition is not ideal when the very small particles are present.

Table 2.11. Particle count results for the mixed samples used in specificity testing. Results for both injection volumes and standard mixes (Stock 1 and 2) are shown. The % difference from the target (target concentration expected for the Stock suspension) was also evaluated.

Sample	Injection Vol (mL)	Total Counts/mL at 2 µm	% Difference from target	Total Counts/mL at 15 µm	% Difference from target
Stock 1 Target particle counts: 2µm=200p/mL, 15µm=800 p/mL	1	203	1.67	669	-16.4
	1	194	-2.84	504	-37.0
	5	209	4.66	482	-39.7
	5	207	3.64	474	-40.8
Stock 2 Target particle counts: 2µm=800p/mL, 15µm=200 p/mL	1	769	-3.83	161	-19.7
	1	766	-4.25	151	-24.5
	5	811	1.33	130	-35.0
	5	796	-0.47	125	-37.5

2.1.3.5 Robustness

Since the HIAC is a light obscuration based system, air bubbles will be detected as particles, making degassing a critical step during sample preparation. Samples were evaluated for the best mode of degassing and the amount of time needed for sufficient degassing of the solutions. Degassing conditions included letting the sample sit at ambient conditions, sonication or exposing to vacuum.

Sample types included two standard formulation buffers (Form A and Form B) commonly used during biotherapeutic product development, particle free water and Form

B with 10 mg/mL BSA added. The buffer formulations had viscosities similar to water. Samples were manually shaken with 30 inversions to introduce air to the system.

A common method for degassing is to let samples sit under ambient conditions for a specified period of time. The results for the samples allowed to sit include the T0 or initial particle counts for comparison to each sample type. It was determined that for some of the samples, at least 5 min sitting would be needed for appropriate degassing. Results for all sample types, with sitting, are shown in Figure 2.3. Sonication was an effective method for degassing and provided low counts after 30 seconds for most samples as shown in Figure 2.4, but it is not recommended for protein solutions since it can be aggressive enough to induce some aggregation. Vacuum degassing provided consistent and low particle counts for all sample types after 30 seconds, and is gentle on protein solutions (Figure 2.5).

Figure 2.3. Particle counts for all samples, degassing by allowing the sample to sit unperturbed. The error bars represent ± 1 standard deviation, N=3.

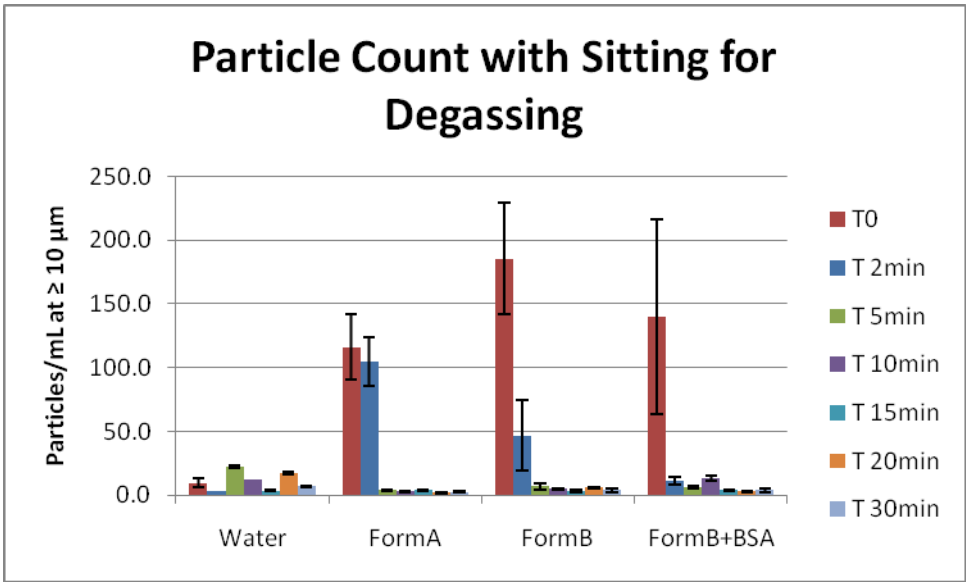

Figure 2.4. Particle counts for all samples, degassing through the use of sonication. Particle count values are included since the values are very low for most samples. The error bars represent ± 1 standard deviation, N=3.

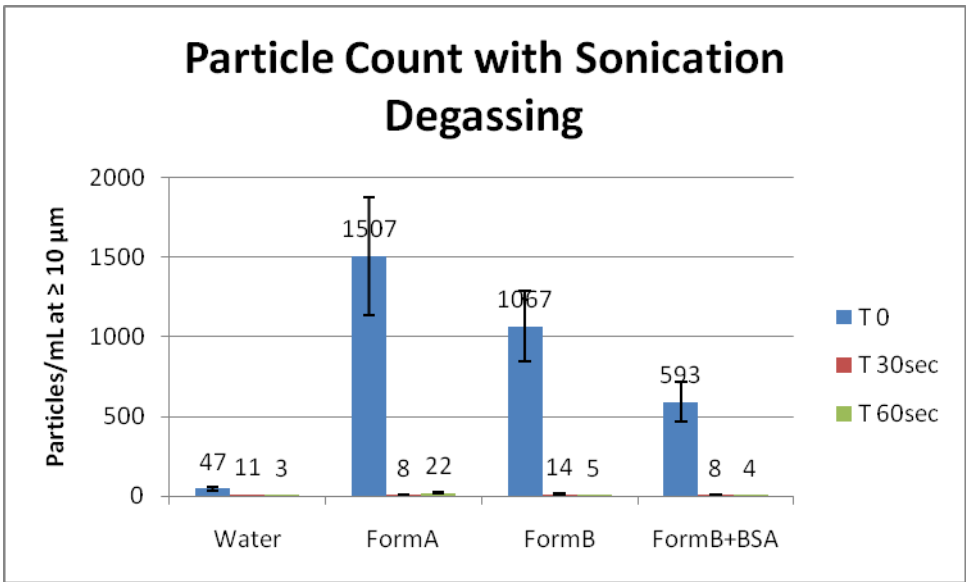

Figure 2.5 . Particle counts for all samples, degassing through the use of vacuum. Note that all counts are very low, even at 30 sec. The error bars represent ± 1 standard deviation, N=3.

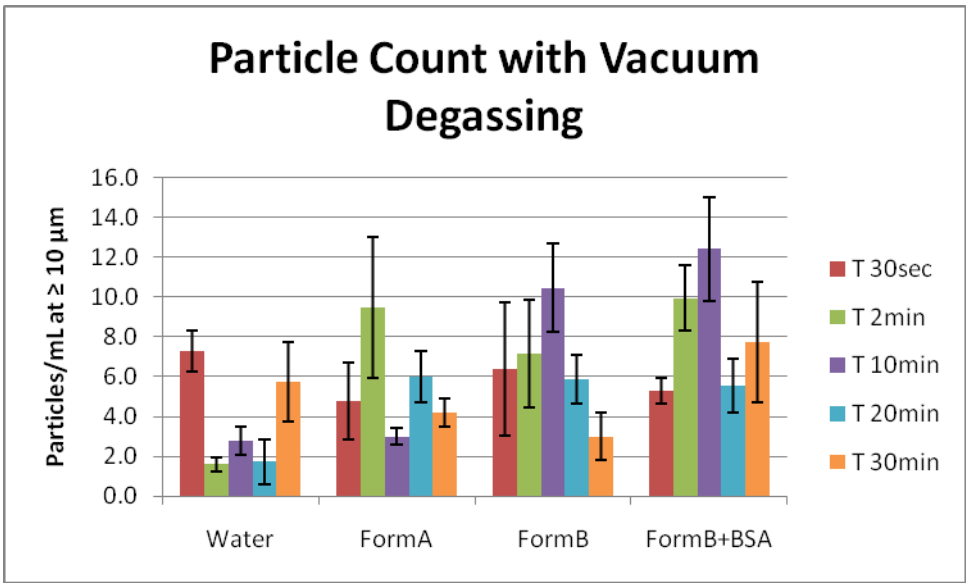

2.1.4 Discussion

The 1 mL injection was shown to be equivalent to the 5 ml injection volume under the test conditions used. The 5 mL injection volume is the accepted volume per USP<788>. This study demonstrates that using a smaller volume, down to 1 mL per injection during sub-visible particle analysis, would provide comparable results.

Specificity studies using mixtures of 2 and 15 µm particles were used to evaluate the effect of mixed particle size distributions on count accuracy. The results indicated that,

in the presence of small particles, larger particles were undercounted. This phenomenon occurred at 1 mL and 5 mL injection volumes and with different ratios of smaller to larger particles. This finding was unexpected and will be investigated in the future. It suggested that the detection mechanism (based on light obscuration) can be affected by the presence of very small particles.

During the sample preparation, it's important that proper degassing is employed. It should be noted that more time may be needed for high concentration and more viscous samples. When not using standard formulation buffers at low protein concentration, it is suggested that a quick degassing study be performed to ensure the amount of degassing is appropriate for the sample type. When there is not enough sample for this type of study, it is suggested that 2 minutes of vacuum degassing be used. A quick check under low magnification using an optical microscope to determine if the test solution is free from bubbles can also be performed. If larger bubbles are still present, additional vacuum degassing may be required.

In summary, the method recommended would utilize the laboratory conditions and environmental checks as described in USP<788>. A 1 mL injection volume would be employed, with 4 injections made, discarding the first. The sample would be prepared by vacuum degassing for 2 min before analysis. Data would be collected from 2-100 μm, with an appropriate system calibration performed before analysis.

2.1.5 Summary

The studies outlined in this section demonstrated the acceptability of monitoring particle counts using a lower injection volume than indicated in USP<788>. In addition, the parameters described allow for collecting particle count information in the 2-10 μm size range. The parameters tested indicated this approach was accurate, linear, precise and robust over the 2-100 μm size range using a 1 mL injection volume. The specificity of particle counting should be investigated further, probing the effect of having very small particles present in a sample. This phenomenon could account for some discrepancies between light obscuration and micro-flow imaging when analyzing protein solutions, where it is common to detect a great deal of very small particles.

2.2 Understanding the Effect of Particle Transparency on Particle Count Differences Between Micro-flow Imaging and Light Obscuration.

Protein aggregation and the presence of particulate matter are of great interest during the development of biologic drug products. There has been much interest in the characterization of protein particles, particularly in the sub-10 μm size range. There are two popular techniques for obtaining particle count information in this size range: light obscuration and dynamic flow imaging. There are, however, significant differences in the particle count results when comparing these techniques. It is believed that these differences are primarily due to the transparency of protein particles, suggesting that dynamic flow imaging is more sensitive to detecting these types of particles. A study was performed to further investigate this phenomenon, using stable standard materials with varying refractive indices (a measure of transparency). In addition, the materials

tested have differences in morphology, so this variable could also be studied for its effect on detection when evaluating these two counting techniques. The results suggest that both particle transparency and particle size play a role in the detection differences between light obscuration and dynamic flow imaging. Particle morphology does not seem to have any effect. Dynamic flow imaging provides a good orthogonal method for the characterization of sub-visible particulates, but caution must be applied when comparing to light obscuration results, especially when analyzing sub-10 µm semi-transparent particles.

2.2.1 Introduction

Protein aggregation is of great interest and concern in the development of biologic drug products. Recently, there has been a lot of discussion around the characterization of particles in the sub-visible size range, with growing interest in the particles that are below 10 µm. The heightened interest in characterization is supported by lack of data around the immunogenic effects of sub-visible protein particles in drug products [22]. To date, there is no particular property of a protein that can be identified as an obvious predictor of immunogenicity, however aggregation leading to protein particulates has been the focus of many recent discussions in this area [23]. Protein aggregate particle size can be categorized into three major size classifications as shown in Figure 2.6. Three classes of particle size ranges were chosen to minimize the number of categories used when discussing particulate matter. Furthermore, the size ranges per class described in this paper, are grouped based on the characterization techniques that might be employed, and their analytical limitations. The technologies available for size and count

characterization, based on their limits of detection, fall nicely within these size ranges. The sub-micron class is usually characterized using techniques such as size-exclusion chromatography (SEC) and dynamic light scattering (DLS), and much more recently, nanotracking instrumentation. The sub-visible particle size class is usually characterized by techniques such as light obscuration, dynamic flow imaging, optical microscopy and electrical resistance (eg., Coulter Counter method). The visible class is usually characterized by visual inspection, but can be analyzed using light diffraction to obtain particle size distribution information, and optical microscopy techniques for obtaining particle size and count, as well as some compositional information.

Figure 2.6. Schematic showing the three ranges that particle size can be divided into. This classification aids in the ability to quickly label a particle group and determine the best characterization approaches to use. The circled region encompasses the sub-visible to visible range, which is the focus of this report.

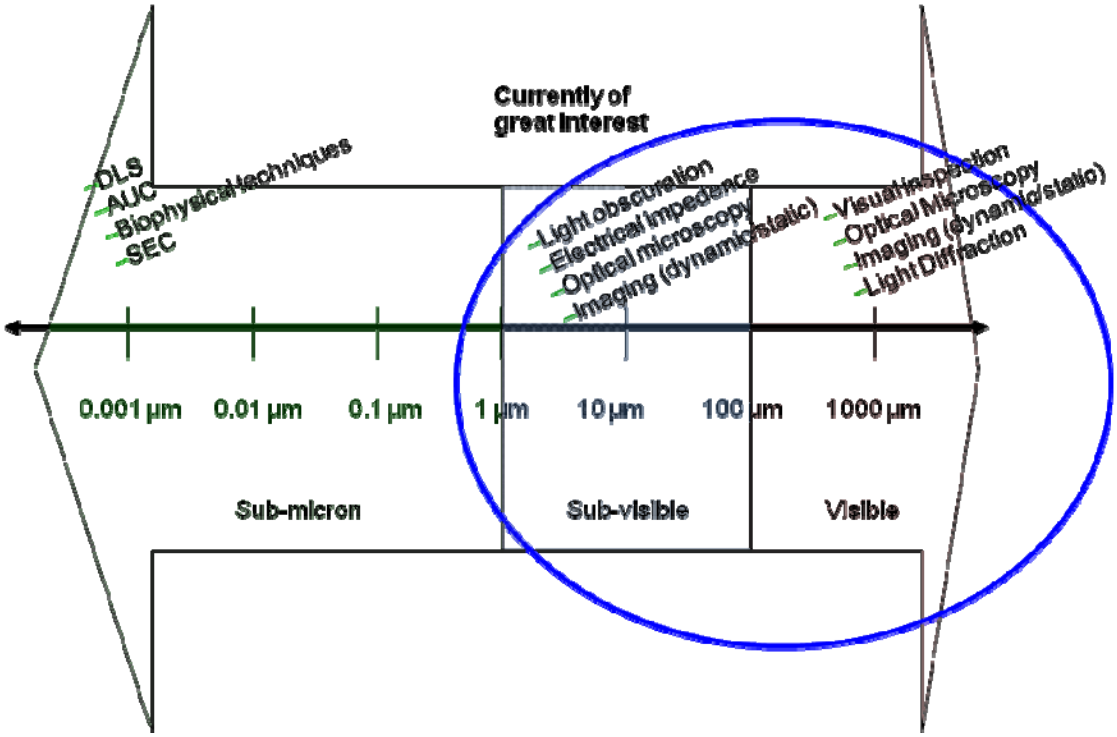

There have been many studies comparing the sub-visible particle counts from two primary techniques, dynamic flow imaging and light obscuration. These techniques are used routinely to analyze biologic drug product formulations for particle load at specific size ranges [24]. Dynamic flow imaging involves a sample flowing past a field of view within a magnification system. Digital images of the sample are captured and analyzed in real time. A popular instrument used for flow imaging is the Brightwell Micro-Flow

imaging system. Light obscuration particle count analysis is an established method, cited in several compendia as the means for obtaining sub-visible particle counts. A popular instrument used for light obscuration is the HIAC instrument.

All the techniques cited earlier have limitations with the method of analysis for protein particles. For instance, it has been shown repeatedly that there is a discrepancy between counts obtained by dynamic flow imaging and light obscuration [25, 26]. Several factors can affect the sensitivity of detection and resulting particle counts for these particle analyzers, including sphericity of the particles, transparency and fragility to shear stress. A popular explanation for the count differences is that the flow imaging systems are better able to detect semi-transparent particles with better sensitivity than light obscuration [27]. There are some contradictions in the literature to this hypothesis, where transparency did not seem to affect particle counts for all studies performed.

Both the dynamic flow imaging and light obscuration techniques are dependent on the interaction of light with the medium the particles are suspended in, as well as the particles themselves. In these instruments, light can be considered as waves that will travel at different speeds through different media. In addition, the light will interact with the particles causing some degree of change in speed of propagation, as well as bending during transmission through the particle, and reflection from the particle. The index of refraction is used as a description of this interaction between light and the particle. The transparency of a particle is related to its refractive index.

Refractive index is defined as:

n = velocity of light in a reference medium / velocity of light in medium of interest

This light is transmitted. Another interaction of light with an object is reflection. The amount of light reflected off an object is related to its reflectivity (R).

The reflection parameter (R) is defined below, and is based on a normal incidence angle and is dependent upon the refractive indices of the object (n_1) and the medium it's in (n_2). For common glass in air (n_1= 1, n_2=1.5) there's about a 4% reflection of the light. This interplay of light and objects, or particles for our purposes, demonstrates that there are several parameters which will affect how a particle is detected in a system based on light interaction.

$$R = [(n_1-n_2)/(n_1+n_2)]^2$$

The standard way to calibrate a particle counting system is to use latex microspheres, with a refractive index of 1.51. It has been reported that a protein particle can have refractive indices ranging from approximately 1.39 to 1.45 [28]. The refractive index is related to how transparent a particle will appear to the counting instrument, and will vary with protein particle properties such as degree of hydration and overall size and shape of the particle.

In this study, we attempted to investigate the effect on detection by dynamic flow imaging and light obscuration using standard materials with very different refractive indices. Standard materials that mimic the optical properties of proteins are not currently available, and protein particles were not used since their properties, such as size and morphology, can change during analysis. It was desired to choose standard materials that were stable and dispersible in aqueous media, within an acceptable size range, and of varying refractive indices. The refractive index values for protein particles range from approximately 1.39 to 1.45, so for this study we chose materials with similar as well as significantly different refractive indices. The standard particles analyzed were stable and not affected by shear forces. Particle shape also varied for these materials and must be considered when evaluating the results.

The standard materials were analyzed using both the HIAC and Brightwell instrumentation. Differences in particle counts were evaluated for each instrument. In addition, the variability for chosen size ranges was also evaluated, as a function of the standard particle physical properties. Based on the current thinking, a sample with a large difference in refractive index from its suspending media, should provide similar results whether analyzed using a HIAC or Brightwell. This assumes that particle transparency is the primary factor in the discrepancies seen with these two instruments.

2.2.2 Materials and Methods

2.2.2.1 Materials

The HIAC/ROYCO model 9703 particle counter (Hach Ulta), equipped with a HRLD-150 sensor was used for all light obscuration analyses. For dynamic flow imaging, the Brightwell DPA4200 (Brightwell Technologies, Inc., Canada) was used throughout. Particle free water (MilliQ) was used for all system flushing and for environmental checks (refractive index 1.33). Phosphate buffered saline, 1X at pH 7.2 (Gibco) was used as the suspension media for the silicon carbide and kaolin materials. NIST traceable Count-Cal polystyrene microsphere standards with a 15 μm nominal diameter (purchased from Thermo-Fisher) were used (these particles have a refractive index of 1.59 at 589 nm). Kaolin, NIST standard #8570, was used (with a refractive index of 1.56). Silicon carbide, standard #F1200-93 (Sympatec) was also used as a standard test material (with a refractive index of 2.55).

A table of the properties of the reference materials is shown below for ease in comparing the materials.

Material	Refractive Index	Primary Particle Size Range	Morphology
Polystyrene microsphere	1.59	15 um monomodal	Spherical
Kaolin	1.56	1-10 um	Plate like
Silicon Carbide	2.55	2-20 um	Irregular, laths

2.2.2.2 Preparation of Standard Solutions

The latex microspheres come as a well characterized suspension with a certified particle count of 3000 particles/mL. This material was used as-is from the container.

Kaolin and silicon carbide were provided as dry powders. Suspensions of each material were made, taking care to keep the concentrations low enough to not saturate the detection systems on either the HIAC or Brightwell instruments. Samples were dispersed in 1X PBS. Initially, the suspensions were prepared at 1.5 mg/100mL. These samples proved too concentrated for the detection systems for both HIAC and Brightwell. This stock suspension was further diluted 1:100 to provide the working suspensions used in the study. Since the long term stability of the suspensions was not investigated, the suspensions were used within 24 hours of preparation and the samples were checked by optical microscopy at the beginning and end of the study.

2.2.2.3 Optical Microscopy

All samples were examined by light microscopy using a Nikon Eclipse ME600 microscope to assess the dispersion properties as well as particle size and morphology. Images were captured and analyzed using a Spot Insight CCD camera and ImagePro Plus software.

2.2.2.4 Light Obscuration

Samples were analyzed using a Hach HIAC, model 9703 light obscuration instrument. Particle size was monitored to cover the range from 1.5 to 100 μm. Samples were tested using 4 runs, discarding the first run. An analysis volume of 1 mL was utilized per run.

2.2.2.5 Brightwell

Samples were analyzed using a Brightwell model DPA4200 micro-flow imaging system. An analysis volume of 1 mL was used for all samples. The illumination of the system was optimized using the 1X PBS diluent used to prepare the samples. The diluent was filtered through a vacuum filtration unit containing a 0.2 μm cellulose acetate membrane, before use.

2.2.3 Results

It has been previously reported that the largest differences in particle counts between the dynamic flow imaging systems and light obscuration lies in the <10 μm size region [29]. Furthermore, it has been suggested that the Brightwell may be providing higher counts versus the HIAC due to attrition of aggregated protein particles, creating smaller particles

that account for the higher differences between techniques at the lower particle size [27]. Samples containing protein particles have been studied most. It's been shown that protein particles vary in transparency with particle size and method of generation [27]. However, the transparency values reported are based on the intensity results obtained using the Brightwell software. It's important to note that these small particles, less than 10 μm and even more significantly for less than 5 μm, will have very limited resolution using a dynamic flow imaging system. For this study, the standard materials tested were evaluated using the Brightwell and HIAC, but were also characterized using static optical microscopy. The materials used in this study were chosen to help probe the idea of particle attrition since these particles are not changing in solution nor are they going to be susceptible to the low shear forces applied during analysis using either technique. The particles tested in this study were in the size range of most interest (less than 10 - 15 μm).

As stated previously, the standard materials were chosen for their differences in physical properties including refractive index. Kaolin and the latex microsphere standards have similar refractive indices but differ in morphology. Silicon carbide has a significantly different refractive index and morphology than the other two standards.

Optical microscopy was used in the characterization of these standard materials. Figures 2.7- 2.9 show the particle characteristics for each standard material tested. As shown, there were differences in the morphology of these particles, with the latex standards being perfectly spherical. The kaolin particles had a plate-like morphology with the majority of the particles in the 1-10 μm size range. The silicon carbide material contained particles

that were irregular in shape, with some small lath shaped particles. These particles were primarily in the 2-20 μm size range. As stated previously, the refractive index values for these samples varied, with silicon carbide having a significantly different refractive index than the other two samples.

Figure 2.7. Photomicrograph of the polystyrene standard material, showing the sphericity of these particles. Sample was tested as-is from the original vial. 200X total magnification.

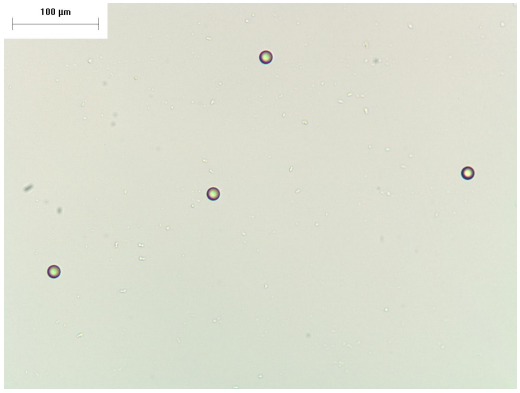

Figure 2.8. Photomicrograph of the kaolin standard material, suspended in the PBS buffer. These particles didn't exhibit a great deal of contrast from the PBS diluent. 400X total magnification.

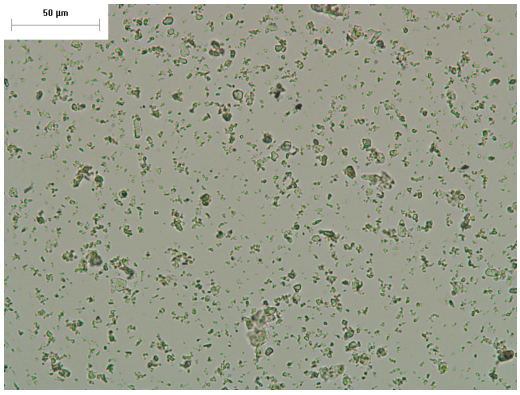

Figure 2.9. Photomicrograph of the silicon carbide standard material, suspended in the PBS buffer. These particles had good contrast from the PBS diluents. 400X total magnification.

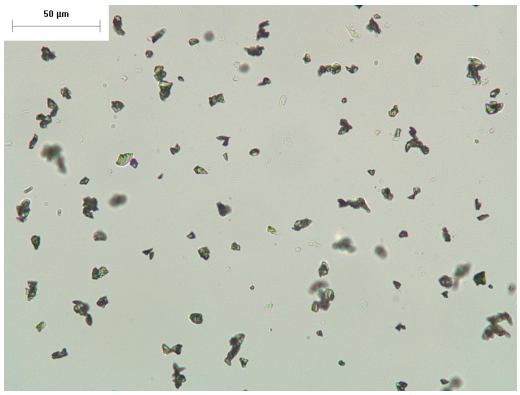

All three standard materials were analyzed by both counting techniques. The particle counts over a broad range of particle sizes were evaluated. The counts for each sample, per size range, were plotted as shown in Figures 2.10 to 2.12. The particle counts for the 15 µm polystyrene microsphere standard were compared using each technique. These particles had a fairly tight monomodal distribution with a nominal diameter of 15 µm. The counts obtained were very similar when looking at the size range encompassing the majority of the particles (10-25 µm). There was some difference at the 1-2 µm size range, with the Brightwell having higher counts. These counts could be due to fines in the sample or other external particulate matter not related to the standard material, but with properties allowing for better detection by the Brightwell. The particle size was too small to be well resolved by the Brightwell imaging system or by optical microscopy. All three standard materials were run in triplicate using each instrument.

The precision of the analyses is shown in Table 2.12. As expected, there was much higher variability with lower particle counts, due to the statistical inaccuracies in small sample sizes. However, it appears that counts obtained per size range for the silicon carbide samples were more variable than kaolin. The polystyrene standard material has low variability by both techniques in the 10-25 μm size range.

The silicon carbide sample (Figure 2.11) resulted in differences between the two techniques, especially in the 2-5 μm size range, where a large population of the particles reside. The kaolin sample distribution (Figure 2.12) resulted in significant differences between techniques when comparing particle counts in the 1-5 μm size range, again where the majority of the particles reside. It should be noted, however, that trends in the size distributions were similar between instruments. The shape of the size distributions obtained by both techniques were similar, but the overall counts differ.

Figure 2.10. Plot of the particle counts per size range for the polystyrene microsphere standard material. Both Brightwell and HIAC results were compared. The error bars represent ± 1 standard deviation, N=3.

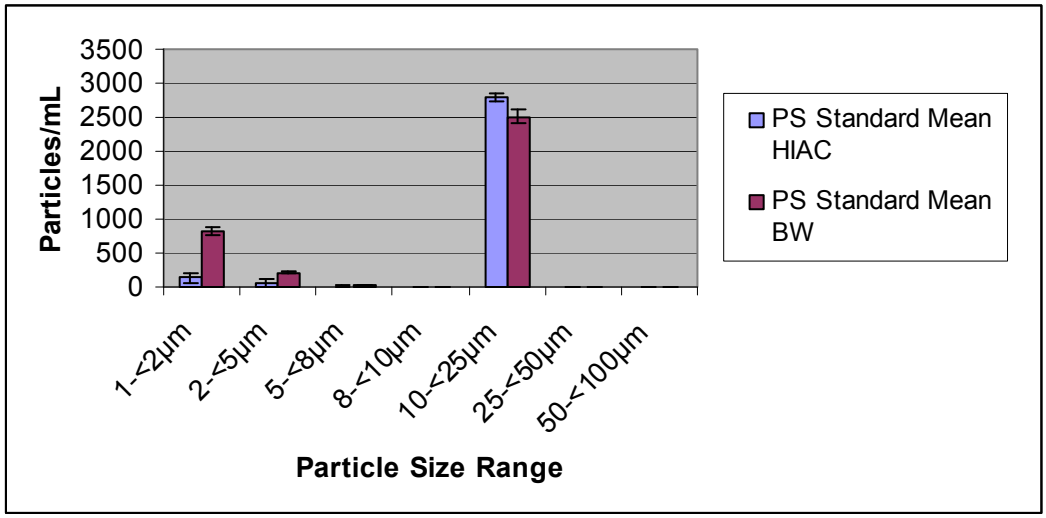

Figure 2.11. Plot of the particle counts per size range for the silicon carbide standard material. Both Brightwell and HIAC results were compared. The error bars represent ± 1 standard deviation, N=3.

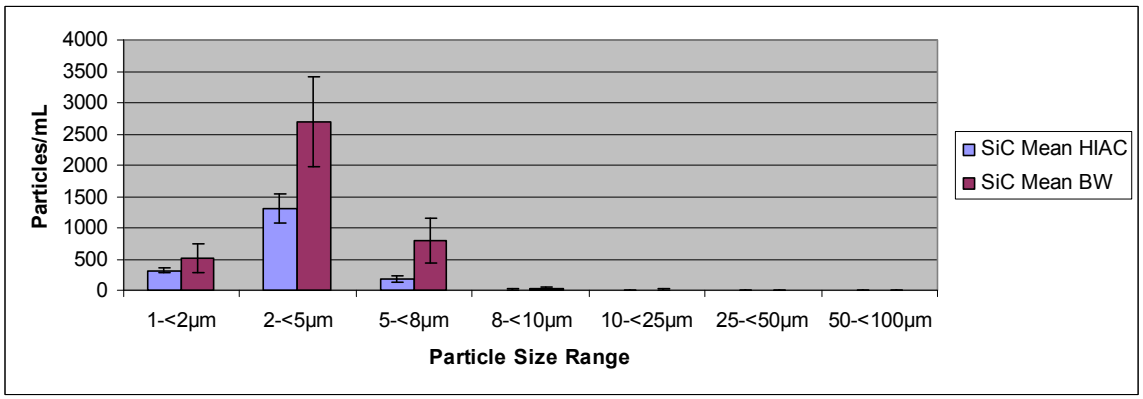

Figure 2.12. Plot of the particle counts per size range for the kaolin standard material. Both Brightwell and HIAC results were compared. The error bars represent ± 1 standard deviation, N=3.

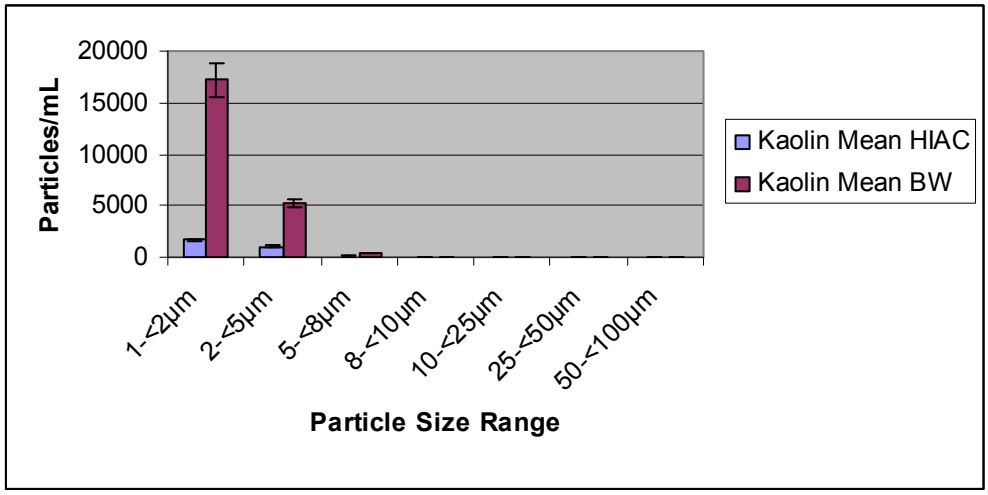

Table 2.12. Precision of count measurements for all standard materials tested. Counts were classified by particle size range. Results for both the Brightwell and HIAC are listed. N=3.

Particle Size Range - HIAC	Mean SiC particles/mL (N=3)	%RSD	Mean Kaolin particles/mL (N=3)	%RSD	Mean PS Standard particles/mL (N=3)	%RSD
1-<2µm	319	11	1705	4	134	58
2-<5µm	1312	17	1062	12	62	77
5-<8µm	180	35	88	21	14	93
8-<10µm	10	44	11	31	5	40
10-<25µm	5	26	8	11	2805	2
25-<50µm	0	N/A	0	N/A	3	67
50-<100µm	0	N/A	0	N/A	0	N/A
Particle Size Range - Brightwell						
1-<2µm	513	43	17271	10	824	9
2-<5µm	2695	26	5231	8	214	4
5-<8µm	796	44	325	5	26	19
8-<10µm	31	34	38	25	3	33
10-<25µm	12	44	27	39	2513	5
25-<50µm	0	N/A	2	100	2	50
50-<100µm	0	N/A	1	173	1	100

Although counts obtained by the Brightwell were higher in each case, the magnitude of that difference varied with the type of sample tested. Table 2.13 lists the absolute difference in counts, per size range, for each sample, as a ratio of the Brightwell results to the HIAC results. These differences were also represented graphically, as shown in Figure 2.13. As seen in the plot, there was approximately a 10 fold higher count obtained for kaolin in the 1-2 μm size range when comparing the Brightwell to the HIAC. This difference was about 6 fold for the polystyrene standard and less than 2 fold for the silicon carbide material. These results are explainable since the silicon carbide had the highest refractive index and should provide better contrast against the surrounding media. The difference continued to decrease as the particle size increases. This data suggests particle size and refractive index play a role in how the particles are detected by the two instruments.

The results obtained using these standard materials suggest there are differences in the two counting techniques, and the difference appears to be dependent on particle size, with lower sizes having larger differences. However, it also appears that as the particle refractive index increases, the difference in counts between the techniques decreases at lower sizes. As the particle refractive index increased, the contrast to its surrounding media also increased.

Table 2.13. The absolute differences in mean particle counts (as a ratio of Brightwell to HIAC particles/mL) per size range (N=3). Note the decreasing magnitude in count difference as the particle size increased.

Size Range	Silicon Carbide	Kaolin	PS Standard
1-<2µm	1.6	10.1	6.1
2-<5µm	2.1	4.9	3.5
5-<8µm	4.4	3.7	1.9
8-<10µm	3.2	3.4	0.6
10-<25µm	3	4	0.9
25-<50µm	0	2	0.7
50-<100µm	0	1	1

Figure 2.13. The absolute differences in counts per size range for all three standard materials. Difference shown is the ratio of Brightwell to HIAC results. The graph shows how differences are minimized with increasing particle size.

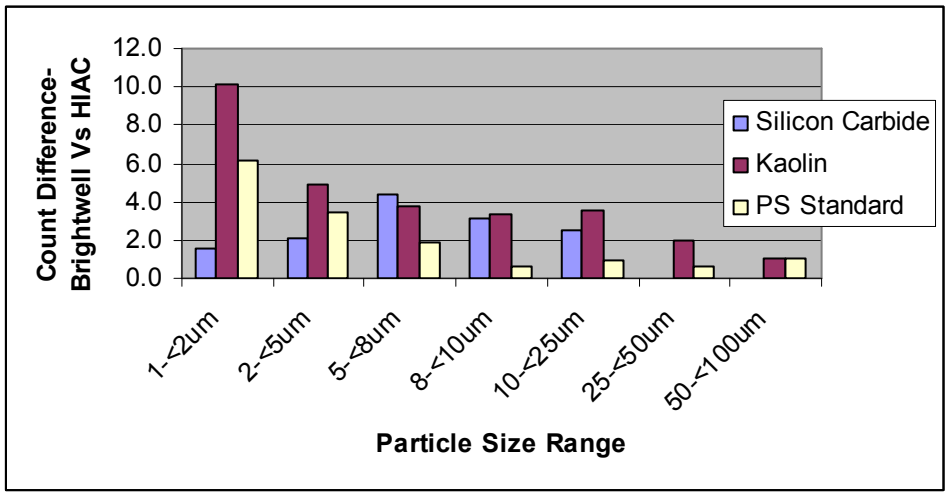

The particle morphology does not appear to play a significant role in the count discrepancies. Differences in the precision of the measurements when comparing silicon carbide and kaolin were observed. A larger sample size would need to be tested to determine how significantly the precision of the measurement is affected by particle type, using both instruments.

2.2.4 Discussion

Differences in particle counts for all standard materials tested were largest in the <10 µm size range. The differences between the Brightwell and HIAC were more pronounced as the refractive index of the particle approached that of the media it was suspended in. Particle shape was not a significant factor, when comparing spherical and more plate like morphologies.

The variability observed with silicon carbide may be due to the high refractive index of this material or may be due to the particle shape. Further investigation is needed to understand this phenomenon and ensure that the dynamic imaging system used can detect particles of interest, regardless of shape or optical properties. Especially in the cases where the data obtained from these systems is being compared to light obscuration results.

It should also be noted that interesting findings were obtained during development of the low volume light obscuration method using the HIAC, as discussed previously. In the

specificity study, 2 and 15 μm particle mixtures were created to evaluate the effect of mixed particle sizes in count accuracy. The results indicated that, in the presence of small particles, larger particles were undercounted, regardless of the injection volume or ratio of amount of small to larger particles tested. The results suggest that having very small particles in the sample can alter the detection efficiency in light obscuration methods. Particle size/count standard materials, such as latex microspheres, are very well defined. The majority of the particles in the sample are within the size range specified on the label. For instance, with a 15 μm standard material, the great majority of particles will be around that nominal size value. Protein solutions, however, have a large population of very small particles (1-2 μm) as regularly detected using flow imaging. These very small particles could interfere with accurate counting using a light obscuration technique. This may play a bigger role in particle count discrepancies observed between light obscuration and dynamic imaging versus the transparency or refractive index of a particle. Future studies will be performed to better understand the effect of large populations of very small particles on the counting efficiency of larger particles.

2.2.5 Summary

Dynamic flow imaging (eg., Brightwell MFI) can be used as an orthogonal technique for light obscuration (eg., HIAC) in obtaining sub-visible particle count information. The results obtained with these techniques might not agree in absolute counts but, in most cases, the trends in counts over a range of particle sizes will be similar. In addition, flow

imaging can provide additional information on the shape and type of particles tested, which can enhance the data obtained by light obscuration.

Chapter 3. Enhancing the Microscopic Visualization of Protein Aggregates by Using a Protein Specific Dye

3.1 Introduction

There is much discussion around the evaluation of protein particles in the sub-visible to visible size range. This is of particular interest when analyzing biologic compounds due to the lack of data around the immunogenic effects of protein particles in drug products [23]. The range of particle sizes can be categorized as sub-micron, sub-visible and visible, as shown in Figure 2.6. The submicron range includes oligomers and multi-mer aggregates. The sub-visible size range varies depending on the detection system, but in general can be described as particles in the 1-100 μm range. The visible particle size range can be described as particles >100 μm. Visual inspection is traditionally used for detection of visible particles in a sample. Sub-visible particles, however, rely on techniques such as light obscuration and dynamic flow imaging for detection.

Dynamic flow imaging involves a sample flowing past a field of view in a magnification system. Digital images of the sample are captured and analyzed in real time. A popular instrument used for dynamic imaging is the Brightwell micro-flow imaging system. Light obscuration particle count analysis is an established method, cited in several compendia as the means for obtaining sub-visible particle counts, where sub-visible is described here as particles less than 100 μm. A popular instrument used for light obscuration is the Hach HIAC instrument.

Techniques such as light obscuration and dynamic flow imaging can require large amounts of sample for proper analysis. Optical microscopy is traditionally a very material sparing technique, and would be preferred when very little sample is available, as is sometimes encountered during the early development stage of biologic products. Parenteral products have to meet particle load requirements as outlined in the United States Pharmacopeia (USP) <788>. The compendium outlines the use of light obscuration analysis for determining particle counts in the sub-visible region. If the sample fails this testing, an alternative test using optical microscopy should be employed. This is where complications can occur when analyzing protein aggregates. Protein particles are amorphous, and can vary significantly in rigidity and transparency. Many protein particles are very flexible and very transparent, with refractive indices reported in the 1.4-1.5 range. When employing membrane microscopy, the sample is filtered onto a depth filter capturing the particles on the filter surface for microscopic examination. Protein particles will embed in the filter membrane and due to their transparency, can be impossible to detect using standard fiber optic lighting as outlined in the compendia. Protein particles can be difficult to visualize, even when using Nucleopore type filters unless specialized lighting is employed, making the approach difficult, even for the experienced microscopist. At times, very labor intensive isolation techniques are needed to capture protein particles for simple visual examination.

The characterization of particles to determine if they are proteinaceous usually involves additional spectroscopic analysis such as FTIR-microscopy or Raman spectroscopy.

These techniques can be time consuming and may require specialized skills for proper sample preparation. The possibility of enhancing the contrast and identification of protein particles on a filter membrane by using visible dyes was evaluated. Fluorescent dyes such as Nile Red were evaluated but required the use of a fluorescent microscope and particle isolation was not user friendly. Using a visible dye would provide an easy and quick approach for characterization. Here, the dye TBPE (3', 3'', 5', 5''-tetrabromophenolphthalein ethyl ester was evaluated because it has been used for the qualitative determination of the presence of protein in samples [30]. Further research showed the use of the dye for quantitative analysis of the relative amounts of serum and spinal fluid proteins. Two solvents, ethanol and methanol, were evaluated for creating the dye solution, as previously published [31].

The feasibility of applying the dye to enhance contrast of filtered protein particles, which could then be analyzed by image analysis techniques, was also investigated. For this study, a monoclonal antibody (mAb) was used, labeled as mAb A. mAb A was stressed by allowing to incubate overnight at 25 ºC before use.

3.2 Materials and Methods

The visible dye, TBPE (3', 3'', 5', 5''-tetrabromophenolphthalein ethyl ester, Fluka #86778) was used to enhance visualization of protein aggregates (structure shown below). This dye was reconstituted in either ethanol or methanol. A Nikon SMZ8000 stereomicroscope was used for observing samples/filter membranes. All solutions were

filtered using a Millex Durapore PVDF filter unit, 0.22 μm. Protein samples were filtered onto a Nucleopore filter membrane (0.4 μm) for visualization.

Model protein solutions included bovine serum albumin (BSA) and ovalbumin, reconstituted using 1X PBS, pH 7.2 (Gibco).

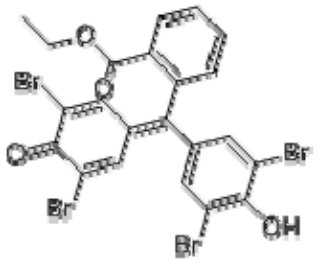

TBPE
$C_{22}H_{14}Br_4O_4$
MW: 661.96 g/mol

Structure 3.1

3.2.1 Preparation of Protein Solutions

A solution of mAb (mAb A) was made at 1 mg/mL in a formulation buffer. This protein solution, greater than 1 yr old, and additionally stressed by placing at 25 ºC overnight, was used. Some visible aggregates could be observed in the solution before use.

3.2.2 Preparation of Dye Solutions

Both methanol and ethanol have been used as diluents for TBPE solution preparation. Both solvents were evaluated to determine which might prove best when adding to protein solutions. Solutions of dye were made at 0.02% w/w dye in alcohol.

It has been shown that protein/TBPE binding was stable for at least 60 min [32]. Although the referenced work used BSA and was performed to determine

spectrophotometric stability, the time during steady color formation was used as a guideline for this study. Dye solutions were added to protein solutions at 1% v/v. All protein/dye solutions made were used within 1 hour of preparation.

A blank dye solution was also prepared using the ethanol dye solution at 10% in 1X PBS. This solution was analyzed by flow imaging to understand the particle counts that might be attributed to a blank sample.

3.2.3 Filtration and Optical Microscopy

When applicable, dye solutions were added to the protein solutions and allowed to incubate for approximately 1 minute before filtration.

Protein solutions were filtered onto the 0.4 μm filter membranes, under clean conditions in a laminar flow hood. Membranes were transferred to cleaned petri dishes and allowed to dry before viewing by microscopy.

3.3 Results

TBPE was chosen as the visible dye to enhance protein aggregate contrast when viewed by microscopy. This dye has been reported to specifically interact with protein, resulting in a colorimetric change [30]. It is believed that the dye interacts with protein through the ester group. The ester, in the presence of the protein particles, has a blue color, thought to be due to the formation of a salt-like adsorption compound, which is not affected by exposure to weak acid. The blue color will persist with proteinaceous particles after being washed with weakly acidic solutions. This reaction appears to be specific for proteins and some alkaloid compounds, when in large amounts. This

specificity makes the dye an ideal candidate for enhancing the visual contrast of protein particles.

Dynamic flow imaging was used to evaluate the interaction of the dye with the model protein systems evaluated. The technique was used to look at the change in particle counts of neat protein solution versus in the presence of dye. The contact time of the dye and protein was relatively short, but any increase in particle counts due to dye interactions were evaluated to ensure it was not inducing aggregate formation.

Table 3.1 lists the particle counts obtained by flow imaging for all particles from 1-100 μm, for all samples tested. Ovalbumin and bovine serum albumin were tested in dye/methanol and dye/ethanol solutions. The methanol solution provided higher counts, suggesting aggregation had occurred. The dye solution in ethanol was also analyzed to confirm background counts. The contribution of dye solution toward particle counts was relatively low, as listed in Table 3.2. This blank dye solution contained very little counts and was not subtracted from any results. The particle counts for each sample were also displayed graphically (Figure 3.1). A review of the results indicated there was instability with ovalbumin when exposed to the dye/methanol solution, as demonstrated by the large increase in particle counts for ovalbumin in dye/methanol when compared to ovalbumin solution in PBS. There was an approximately 2-3 fold increase in particle counts for ovalbumin in dye/ethanol solution compared to an approximately 50-500 fold increase in particle counts for ovalbumin in dye/methanol solution. The dye/methanol solution did not have as acceptable results as the dye/ethanol solution.

Table 3.1. Particle concentrations (particles/mL) for each solution over a range of particle sizes, from 1 to 100 µm.

Size Range	BSA	BSA + dye/methanol	BSA + dye/ethanol	OA	OA + dye/methanol	OA + dye/ethanol
1-<2µm	827	506	739	1410	822246	3328
2-<5µm	370	175	134	419	256938	1431
5-<8µm	35	50	16	152	71356	358
8-<10µm	4	16	4	49	24190	115
10-<25µm	9	31	12	87	34577	175
25-<50µm	2	5	1	13	619	22
50-<100µm	0	0	0	1	11	3

BSA: bovine serum albumin
OA: ovalbumin

Table 3.2. Particle concentrations (particles/mL) for the blank/dye solution in ethanol over a range of particle sizes. Due to the low counts, no blank subtractions were performed.

Size Range	Blank (dye)
1-<2µm	134
2-<5µm	56
5-<8µm	23
8-<10µm	5
10-<25µm	8
25-<50µm	0
50-<100µm	0

Figure 3.1. Particle concentrations (particles/mL) for each solution over a range of particle sizes, from 1 to 100 µm, as determined by flow imaging. Error bars represent 1 standard deviation.

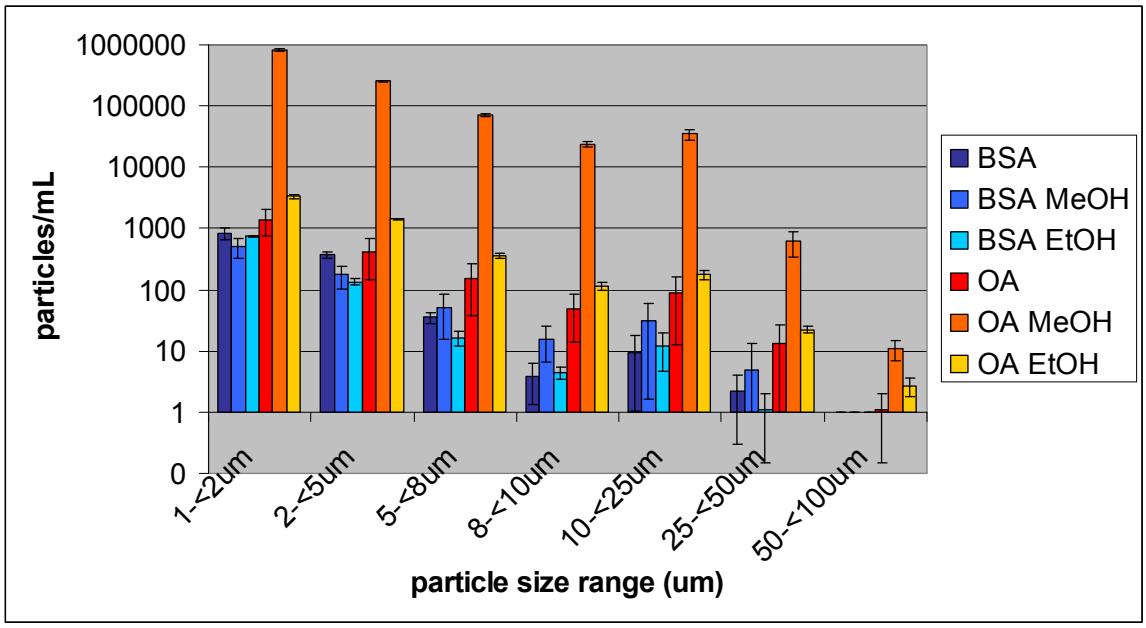

In addition, optical microscopy/image analysis was employed to observe the amount of proteinaceous particles on the filter membrane after exposure to the dye/methanol solution and filtration. Figures 3.2 to 3.5 are images of representative areas on the filter membranes. No particles were detected in the BSA solution (Figure3.4) which agrees with micro-flow imaging results. The ovalbumin sample contained fibrous protein particles. Using microscopy, the elongated fibrous nature of the particles was easily detected.

Figure 3.2. Photo showing the ovalbumin particles on the filter membrane, after exposure to dye/methanol (15X magnification). The fibrous protein particles are easily seen on the filter membrane.

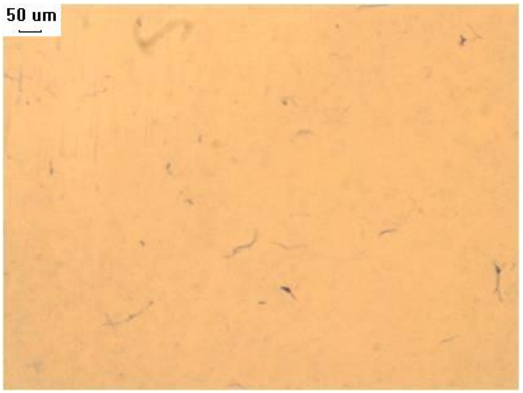

Figure 3.3. Photo showing the ovalbumin particles on the filter membrane (45X magnification)

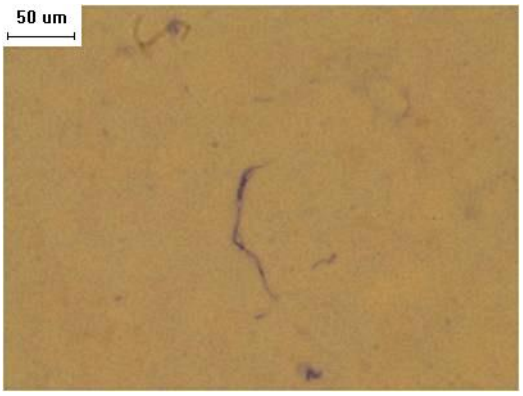

Figure 3.4. Photo showing the lack of particles on the filter membrane for the BSA sample (45X magnification)

Figure 3.5. Photo showing a foreign fiber on the filter membrane under coaxial lighting (75X magnification). The particle is easily identified as a foreign particle due to the birefringence under the coaxial lighting along with lack of dye uptake.

Because it was determined that dye solutions made using ethanol are less stressful to protein solutions, this dye composition was used to evaluate enhanced contrast of mAb A

aggregates after filtration onto a nucleopore membrane. It should be noted that this conclusion using ethanol may not apply to other classes of proteins, and was used for mAb A due to the hydrophobic nature of the surface of this class of proteins. A similar evaluation would be warranted if other classes of protein were evaluated.

Protein aggregates could be seen visually on the filter. The first attempts at an automated detection were performed. The filter was dried and scanned using a BioRad densitometer. The filter image before and after count analysis is shown in Figure 3.6. The filter membrane had a pale blue background with darker blue areas representing the protein aggregates. There was sufficient contrast for the densitometer to detect the aggregates and 'mark' them for counting (dark blue squares on bottom image, Figure 3.6). The system was able to distinguish protein aggregates from background, and provide particle count information in the form of number of blue spots on the filter (519 particles counted). Using a visible dye along with an image analysis technique was a feasible approach for characterizing protein aggregates. Further studies will be performed using more sophisticated image analysis techniques to enhance contrast and analysis of the particle population.

Figure 3.6. mAb A solution, filtered and dyed for enhanced contrast, before (top) and after (bottom) counting the particles.

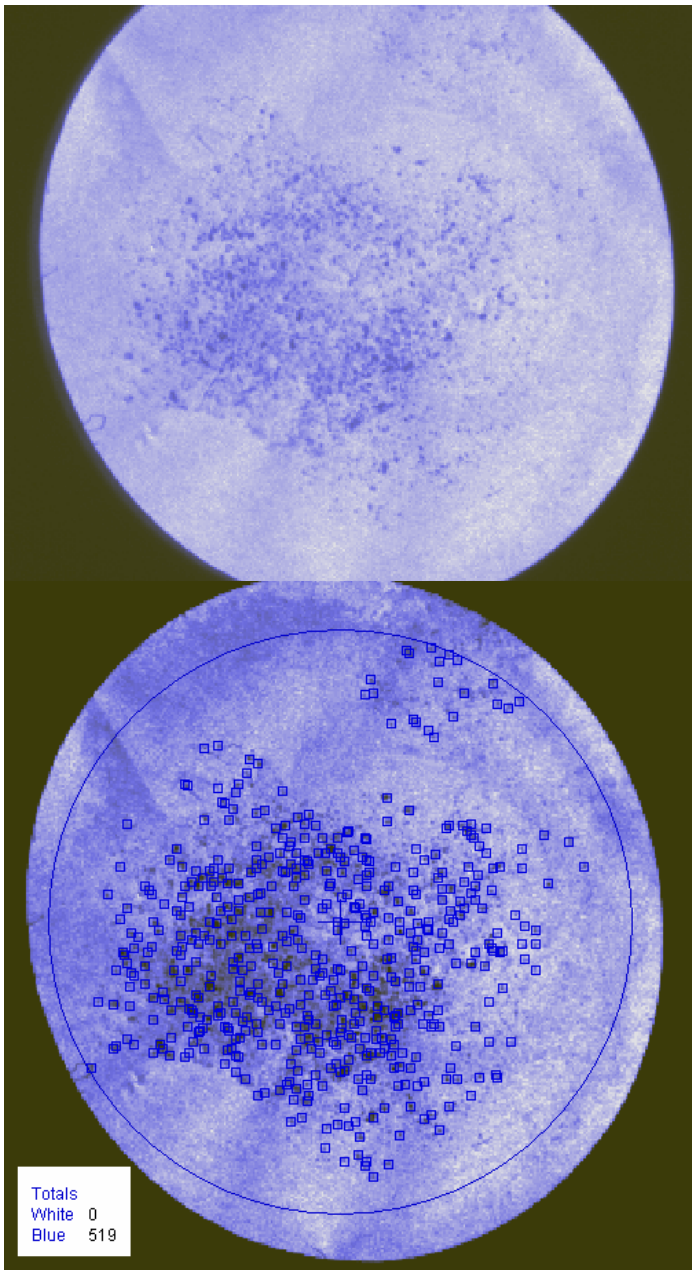

3.4 Discussion

There are many advantages to using a dye to enhance the contrast of protein particles when viewed microscopically. Because of the transparency and flexibility of protein particles, they were not easily viewed on a filter membrane. Adding a visible dye, allowed for quick evaluation of the particle load as well as morphology. In addition, because TBPE is a protein specific dye, it allowed for rapid assessment of whether a particle is proteinaceous. Silicone oil and semi-solid particle contaminants can appear as transparent and flexible particles but will not retain the dye after washing with a mildly acidic solution as has been discussed in the literature and demonstrated in previous experiments (images not provided) [30].

The approach for particle visualization described here can be used as an orthogonal method for light obscuration or flow microscopy, or visual inspection testing. The approach would cover a very broad range of particles sizes, limited only by the magnification achievable with the microscope used.

Another advantage of this approach was the ability to characterize particles using extremely small volumes, as low as a few drops of solution if desired. For the example described, 1 mL of solution was filtered but the upper limit of filterable volume will only be limited by the abundance of particles in the test solution. With very high particle concentrations, it will be necessary to limit the volume filtered to create a monolayer of

particles on the filter membrane. Particulate matter can be captured on a filter membrane for characterization of size, shape and composition.

3.5 Summary

The use of a visible dye to enhance visual contrast and provide an indication as to whether the material is proteinaceous, has been shown to be feasible. This technique allows for rapid analysis of particle abundance, morphology and type.

An area for future investigation will be to apply this approach to the quantitative analysis of protein particles in conjunction with automated image analysis.

Chapter 4. Silicone Oil and Protein Interactions

Impact of silicone oil on protein aggregation formation/ morphology under pharmaceutically relevant conditions

4.1 Introduction

The effect of silicone oil on protein stability is an area that is still under investigation, and not well understood. There have been several reports showing silicone oil has no effect on protein stability, and yet other studies suggest the silicone oil droplets can induce aggregation [33, 34]. It appears that interactions between protein and silicone oil may be dependent upon the protein molecule. A study was performed to look at the effect of protein in the presence of silicone oil droplets (as an emulsified suspension) [35]. It was hypothesized that protein was coating the silicone oil droplets and could affect the zeta potential of these particles leading to increased or decreased stability of the suspension. There was quite a bit of indirect evidence that protein was actually coating the oil droplets including the change in oil droplet size and state of aggregation in the presence of protein. Oil emulsions without protein were found to contain discrete droplets less than 10 μm in size. After exposure to protein, droplets were highly aggregated with an average size of approximately 100 μm. In addition, there was a loss of soluble protein for all formulations after exposure to silicone oil, with no increase in aggregate levels. The findings suggest that protein was coating the oil droplets.

The objective of this study was to investigate the effect of the presence of silicone oil on the physical stability of model proteins, and most importantly, to be able to distinguish between protein particles and silicone oil particles. This study looked at the effect of two proteins, bovine serum albumin (BSA) and ovalbumin, when exposed to silicone oil particles under stressed conditions. BSA is reported to have a higher surface hydrophobicity than ovalbumin, but studies show that the binding of hydrophobic probes is a combination of hydrophobic binding sites and nearby charged residues [36]. The goal was to detect any interaction between protein and the silicone oil particles, and characterize any resultant particles.

4.2 Materials and Methods

4.2.1 Materials

Model proteins were used for this study, including Bovine Serum Albumin (Sigma #A4503) and Ovalbumin (Sigma (#A5503-1G). Both proteins were reconstituted in 1X phosphate buffered saline (PBS), pH 7.2 (Gibco 20012) at 10 mg/mL.

Silicone oil (Dow Corning, 350 CST), 360 medical fluid grade was used throughout this study. Oil suspensions were made in deionized water (1% vol/vol), emulsified before use.

Samples were prepared in 1 mL glass vials (Schott part # 68000313). The vials were washed with particle free water (MilliQ) and depyrogenated. Serum stoppers were used to seal vials as needed. West (# 19560182-S2-F451 R-B2-40) 13 mm stoppers were used

after washing with particle-free water and autoclaving. All the materials used in this study were used and stored under low particulate conditions in a laminar flow hood.

Microscopic analysis was performed using a Nikon ME600 optical microscope equipped with a Spot digital camera and ImagePro image capture and analysis software. Thermal analysis was performed using a MicroCal DSC system. Analysis was performed at a 100 ºC/hr scan rate, over a range of 20-110 ºC. Samples were analyzed at 2.5 mg/mL. SDS-PAGE analysis was performed using NuPAGE polyacrylamide gels and a colloidal blue stain. Both reduced and non-reduced conditions were tested. Gels were de-stained and analyzed using a Bio-Rad GS-800 densitometer. UV spectroscopy was performed using a Nanodrop system. A Brightwell MFI DPA4200 was used for any flow imaging analysis.

4.2.2 Silicone Oil Preparation

To create conditions that are pharmaceutically relevant, the type of silicone oil that a sample would encounter (from a prefilled syringe coating for example) was introduced. In order to dispense and handle the oil, an emulsion was created. The emulsion was found to be stable 30 minutes after preparation, as determined by flow image analysis. The silicone oil emulsion was prepared as follows for all studies performed:

A 1% solution of silicone oil was made in 0.2 um filtered 1X PBS buffer, pH 7.2, in a cleaned plastic conical tube. The sample was vigorously shaken (complete inversions) for 10 sec. The suspension was then subjected to 10 min sonication in a sonic bath. This

was followed by an additional 10 sec of vigorous shaking. The sample was then used immediately when possible, and within 30 minutes of preparation if needed.

4.2.3 Protein Sample Preparation

Care was taken during the preparation of all samples to avoid introduction of foreign particulate matter. All samples were prepared and handled in a laminar flow cabinet and all materials were rinsed with particle free water as necessary to reduce foreign contamination.

Samples were heated at 85 ºC for 15 min with agitation to induce aggregation for visual evaluation.

A 1% silicone oil emulsion was prepared and added to the protein solutions at a 1:1 volume ratio, resulting in an oil concentration of 0.5% in the protein samples.

Sample formulations were prepared as shown in Table 4.1. An appropriate volume of PBS was added to the protein solutions that did not contain silicone oil as a control.

Table 4.1. Formulation details for test samples.

Vial Code	Protein	Protein conc (mg/mL)	1% silicone oil suspension added	# vials
B1	BSA	10	0 (PBS dilution)	1
B2	BSA	10	1:1 with protein	1
O1	Ovalbumin	10	0 (PBS dilution)	1
O2	Ovalbumin	10	1:1 with protein	1
S1	None	0	1:1 dilution w/buffer	1

4.2.4 SDS-Page

SDS-PAGE was performed on the samples, using the components listed in Table 4.2.

Table 4.2. Components used in SDS-Page analysis.

Item	Vendor	Cat #	Lot
Gels- NuPAGE 4-12% Bis/tris 1mmX12 wells	Invitrogen	NP0322BOX	9061276
Sample buffer- NuPAGE LDS sample buffer 4X	Invitrogen	NP0007	555099
Running Buffer/NuPAGE MES SDS 20X	Invitrogen	NP0002	572203
Novex Stainer A, colloidal blue kit	Invitrogen	46-7015	453724
Novex Stainer B, colloidal blue kit	Invitrogen	46-7016	453725

4.2.5 Optical Microscopy

Optical microscopy was performed on the samples to determine the morphology and abundance of particles in the samples. The presence of silicone oil droplets was easily

identified based on shape and optical properties. Samples were examined neat, with no coverslip.

4.2.6 Fluorescence Microscopy

Fluorescence microscopy was employed to aid in the visualization of protein aggregates when formed in the presence of silicone oil droplets. A variety of fluorescent dyes were evaluated including ThioflavinT, ANS, congo red, and nile red. Nile red was found to provide the best imaging properties with longer time before quenching. Nile red was used for all fluorescence studies described. A 1 mM solution of nile red in ethanol was used throughout. It was determined that nile red had very minimal affinity for the silicone oil droplets making it a very useful dye for determining if protein was present when silicone oil was also present.

4.3 Results

4.3.1 Silicone Oil Emulsion

A sample of the silicone oil emulsion was prepared and monitored over time. The emulsion was prepared and evaluated at 30 min. and after 4 days sitting at 2-8ºC. The goal was to allow the emulsion to sit for a prolonged period of time to allow for coalescence/stability and then try to regenerate the particles by introducing energy into the system. The turbidity of the sample was much less than at T0 after 4 days, so the sample was re-sonicated and shaken to recreate the emulsion. This sample was evaluated by dynamic imaging and found to contain a much finer dispersion of particles, very

different from the original emulsion. Fresh emulsion preparations were used in this study, based on this information.

Particle count results for the emulsion samples are shown in Table 4.3. The particle counts for a water blank were included, demonstrating the minimal contribution from the background. Corresponding images for these samples are shown in Figures 4.1 to 4.3. The images indicate that the re-emulsified sample contained much finer particles. There were a great deal more particles generated, with many touching in the images. Crowded images like this can lead to erroneous results, where the analysis software sees the agglomerate of particles as a single unit of larger size. This was reflected in the larger mean size (ECD) value reported for this sample.

It was determined that the prepared emulsion should be used within 30 min. after preparation. This time frame ensured there was a sufficient amount of particles remaining with a desired particle size distribution.

Table 4.3. Particle count results for the silicone oil emulsion at initial and 30 min after preparation. In addition, the results for a water blank and for the re-emulsified sample, after 4 days are included.

			Particles/mL, size range in µm						
Sample	Mean ECD (um)	Total conc (p/mL)	≥1 to <2	≥2 to <5	≥5 to <8	≥8 to <10	≥10 to <25	≥25 to <50	≥50 to <100
water blank	1.8	77	67	7	0	2	2	0	0
1% emulsion in PBS, T0	3.5	13143857	6157661	4604569	1286710	414143	598511	81071	1192
1% emulsion in PBS, T30min	3.3	7895587	3791819	2745598	723397	259252	355908	19432	181
1% emulsion, T4 days, resonicated	7.7	17535293	5822272	4214073	2135652	1015940	3256868	977440	112546

Figure 4.1. Images from the flow imaging system showing the particles detected at each size range for the emulsion at the initial time point.

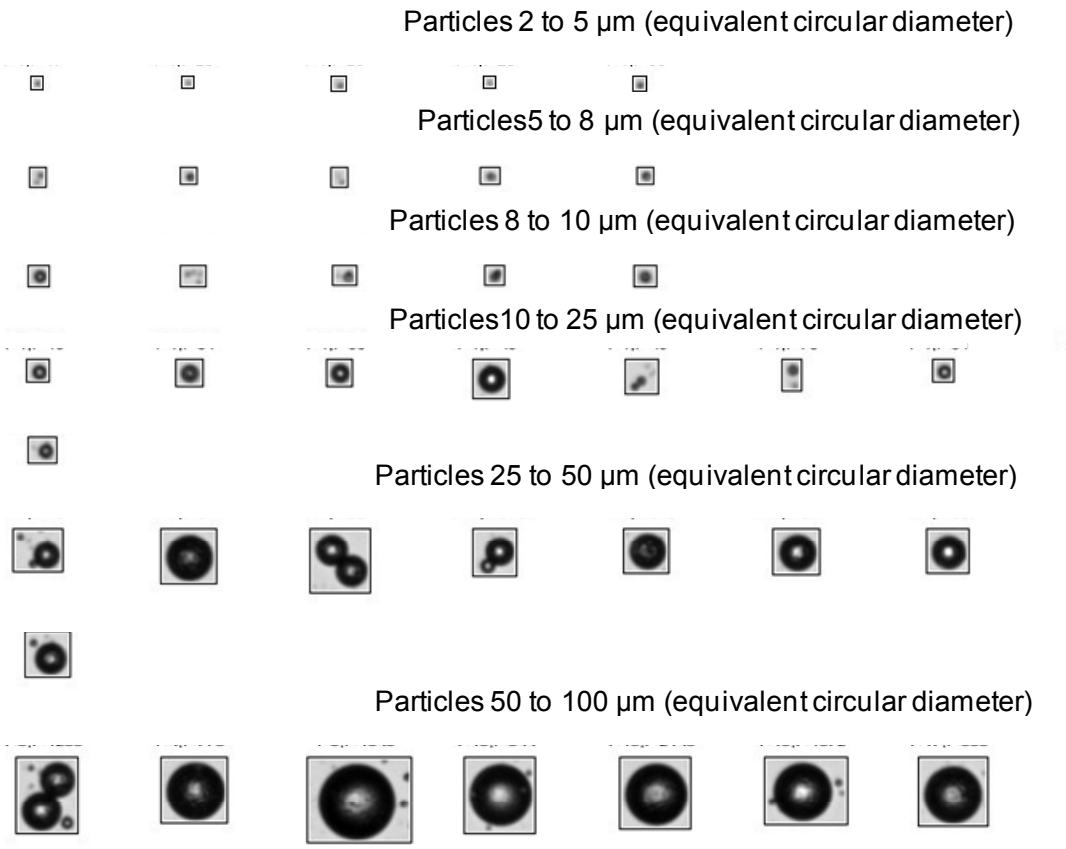

Figure 4.2. Images from the flow imaging system showing the particles detected at each size range for the emulsion at the 30 min time point.

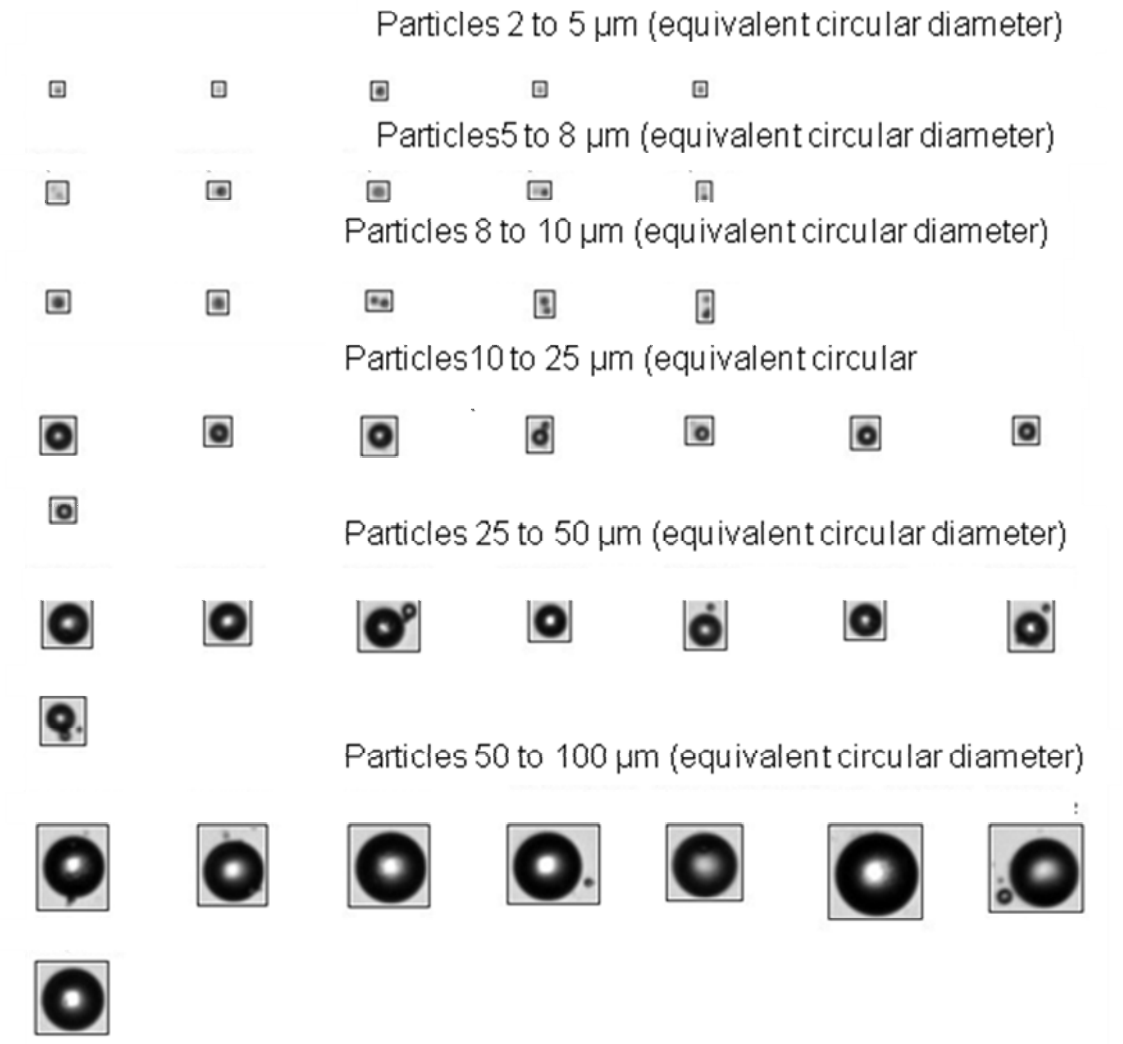

Figure 4.3. Images from the flow imaging system showing the particles detected at each size range for the re-emulsified sample.

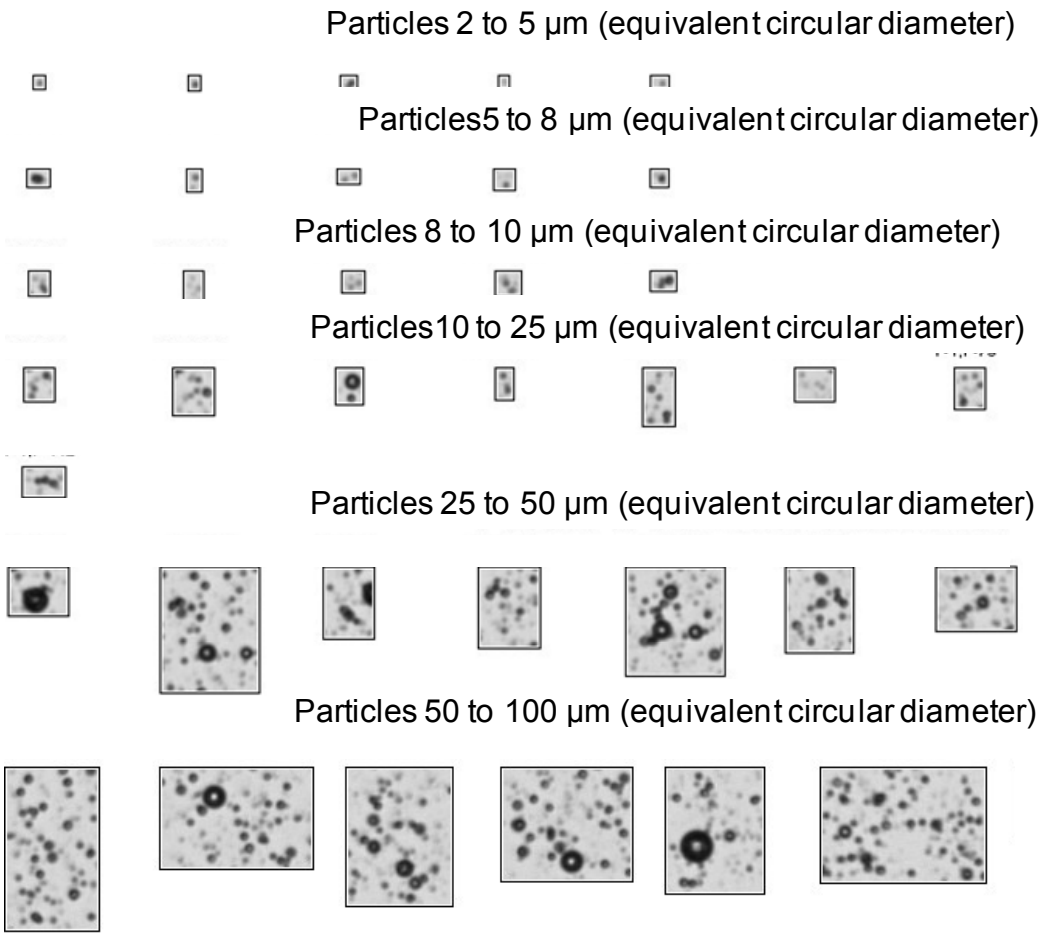

4.3.2 Protein Analysis in the Presence of Silicone Oil

4.3.2.1 DSC

The protein samples were analyzed by DSC to determine if there was any change in the melting temperature (Tm) for the samples in the presence of silicone oil particles. The DSC thermograms are shown in Figure 4.4. A table showing the Tm values for each

sample is shown in Table 4.4. The neat silicone oil emulsion was also analyzed. The results show no effect of silicone oil on Tm values for any of the samples. Sample details are listed in Table 4.1.

Figure 4.4. DSC thermograms for all samples tested.

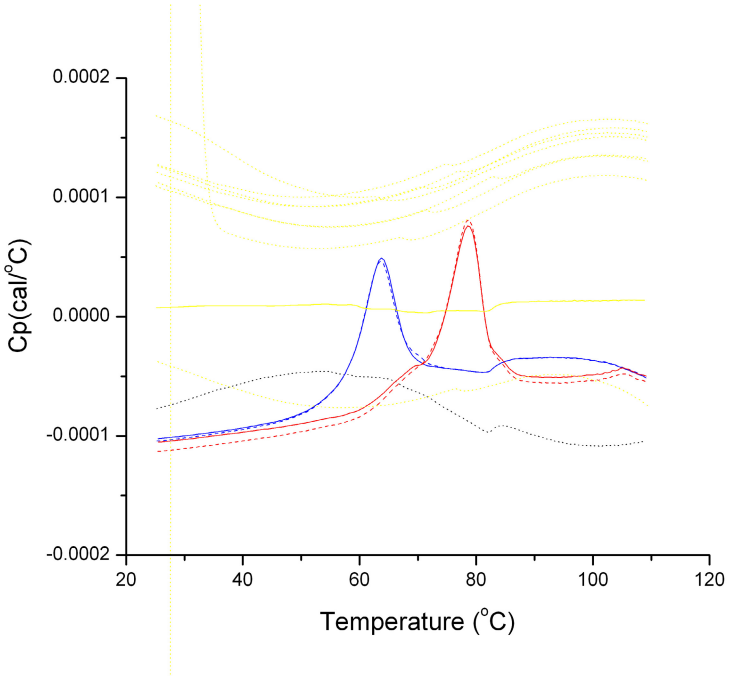

Solid red: (O1) Ovalbumin with no silicone oil
Dashed red: (O2) Ovalbumin with silicone oil
Solid blue: (B1) BSA with no silicone oil
Dashed blue: (B2) BSA with silicone oil
Dashed black: silicone oil suspension
Yellow: blank baselines

Table 4.4. Tm values for all samples tested, including the neat silicone oil emulsion.

Sample	Tm
B1 BSA	63.3
BB2 BSA	63.3
O1 albumin	78.4
O2 albumin	78.4

4.3.2.2 SDS-PAGE

The albumin samples were heated at 85ºC for 15 min with agitation, to induce aggregation. Samples were evaluated in the presence and absence of silicone oil particles and analyzed by reduced and non-reduced SDS-PAGE. Table 4.5 lists the SDS-PAGE results for the samples. The % High Molecular Weight Species (%HMWS) and % parent compound remaining are listed. Figures 4.5 and 4.6 show images of the reduced and non-reduced gels. The first two lanes contain molecular weight markers (Invitrogen cat #LC5677, 12 band marker set), with the molecular weights listed in the image. A silicone oil sample was analyzed as a blank (lane 3).

SDS-PAGE results indicate that there was a significant amount of irreversible aggregation with heating both albumin samples. The larger aggregates were dissociated after adding a reducing agent, suggesting reduction of disulfide linkages. Most importantly, no significant effect of having silicone oil present was observed.

Table 4.5. SDS-PAGE results for the samples, showing the percent calculated for the %HMWS and parent species, determined by densitometry of the colloidal blue stained gels.

Non Reduced		
Sample ID	**%HMWS**	**%Parent**
B1 (BSA)	39	59
B2 (BSA/Oil)	38	59
O1 (OA)	13	78
O2 (OA/Oil)	11	78
B1 (BSA) Heated	>90	<10
B2 (BSA/Oil) Heated	>90	<10
O1 (OA) Heated	57	39
O2 (OA/Oil) Heated	69	28
Reduced		
Sample ID	**%HMWS**	**%Parent**
B1 (BSA)	26	74
B2 (BSA/Oil)	25	75
O1 (OA)	11	86
O2 (OA/Oil)	12	82
B1 (BSA) Heated	34	64
B2 (BSA/Oil) Heated	35	61
O1 (OA) Heated	20	64
O2 (OA/Oil) Heated	21	63

Figure 4.5. Image of the non-reduced gel. The lanes are labeled with the sample name. Non-heated samples are in lanes 4-7, lanes 9-12 on the right-hand side of the gel are the heated samples, in the same order.

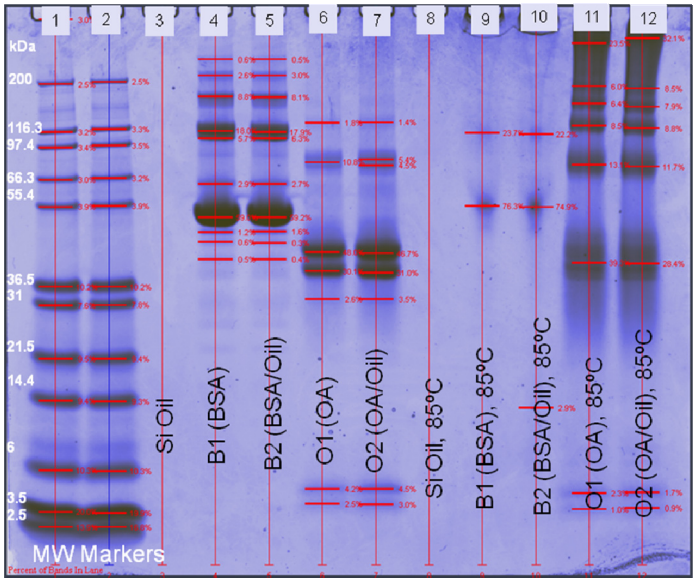

Figure 4.6. Image of the reduced gel, showing the dissociation of aggregates created with heating. The lanes are labeled with the sample name. Non-heated samples are in lanes 4-7, lanes 9-12 on the right-hand side of the gel are the heated samples, in the same order.

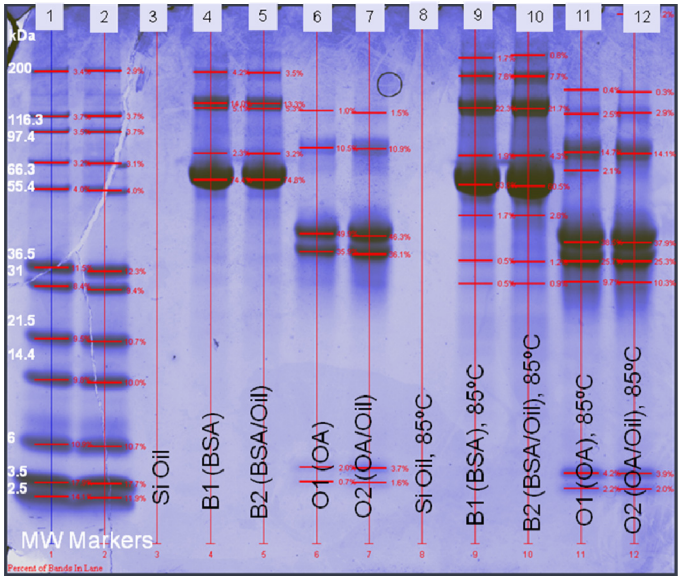

4.3.2.3 Optical Microscopy

Optical microscopy was also performed on the samples to determine the physical state of the samples right before DSC and SDS-PAGE analysis. No aggregates were observed, and silicone oil droplets were easily detected in samples containing the emulsified oil. A photomicrograph of the silicone oil emulsion is shown in Figure 4.7. The oil particles had a broad size distribution. The BSA and Ovalbumin samples, after preparation and before adding silicone oil (no heating), were evaluated with no particles observed (no images provided).

Figure 4.7. Silicone oil emulsion sample, 200X total magnification.

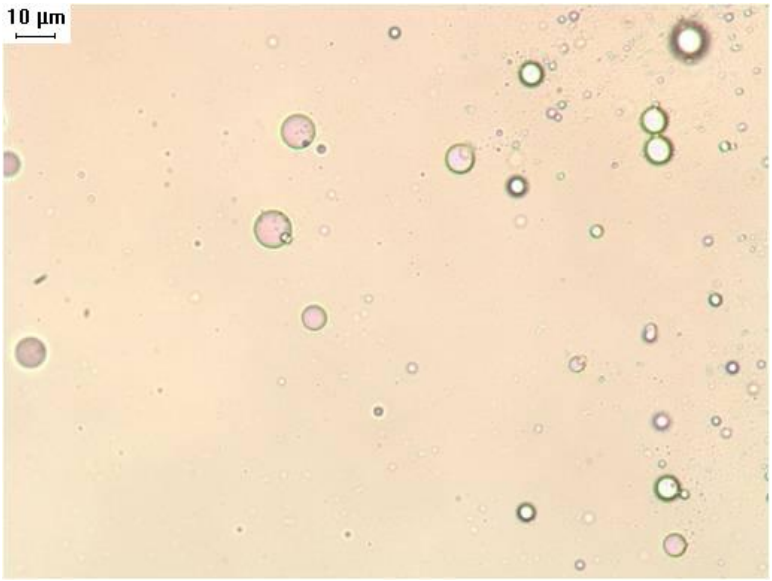

All samples were again imaged after DSC and SDS-PAGE analysis. The proteins had time to sit in the presence of the oil particles. Figure 4.8 shows the silicone oil suspension after sitting. Fine oil droplets are still present, but the larger droplets are no longer observed. The BSA and Ovalbumin samples (no oil added), after sitting, had no observable particles (no image provided). The BSA plus silicone oil sample, after sitting, still contained the oil droplets but no protein like particles were observed (Figure 4.10). The Ovalbumin plus silicone oil sample, after sitting, still contained oil droplets and some small protein like particles. There appeared to be some association of the protein with the oil droplets, a fine coating was seen in some microscope fields (Figure 4.13).

Next, heat was applied to the samples and all were examined again. The silicone oil suspension had the same appearance as before heating (Figure 4.9). The BSA sample, after heating, contained many sheet like and fibrous aggregates, as shown in Figure 4.11. The BSA sample with silicone oil after heating, however, did not contain the fibrous or sheet like particles. Rather, a large number of spherical particles, resembling the silicone oil droplets were observed (Figure 4.12).

The Ovalbumin sample, after heating, was also examined. The sample contained a great deal of sheet like and fibrous aggregates as shown in Figure 4.14. The Ovalbumin and silicone oil sample, after heating, showed a significant change in particle morphology. Some spherical particles resembling silicone oil droplets were seen, and many small, more equant aggregates were observed (Figure 4.15). These particles were examined under higher magnification, and it appeared that the protein had aggregated and was

intimately associated with silicone oil droplets. Figures 4.16 and 4.17 show representative aggregates, demonstrating the association with the oil droplets. Under high magnification, the association between protein and silicone oil droplets was clearly seen. These results indicate the presence of silicone oil can affect the morphology of protein aggregates and must be considered when present during particle characterization studies.

Figure 4.8. The silicone oil suspension after incubation. Fine oil droplets were still present, but the larger droplets were no longer observed. 100X total magnification.

Figure 4.9. The silicone oil suspension sample, after heating. The sample had the same appearance as before heating with an abundance of small droplets observed. 100X total magnification.

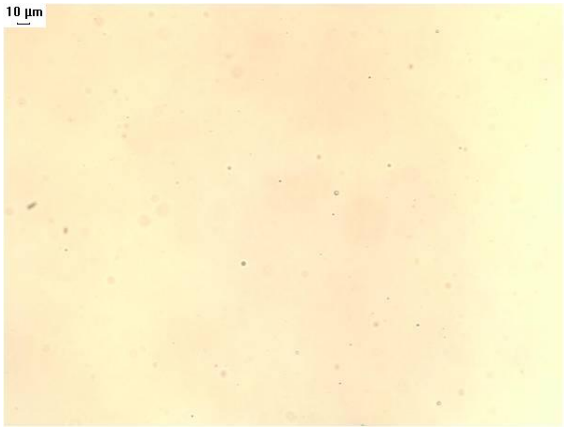

Figure 4.10. The BSA plus silicone oil sample, after incubation, still contained the oil droplets, but no protein like particles were seen. 100X total magnification.

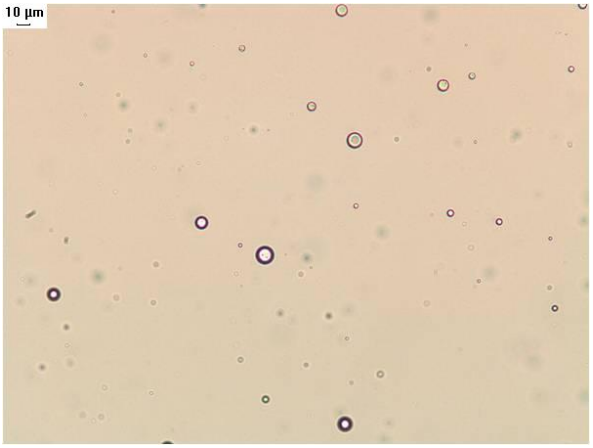

Figure 4.11. The BSA sample, after heating, contained many sheet like and fibrous aggregates. A representative particle is shown. 100X total magnification.

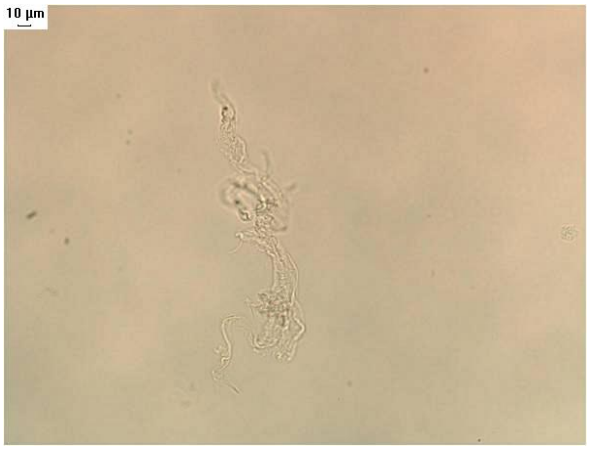

Figure 4.12. The BSA sample with silicone oil after heating. Fibrous and sheet like aggregates were not seen. Spherical particles resembling the silicone oil droplets were observed. Total magnification 100X.

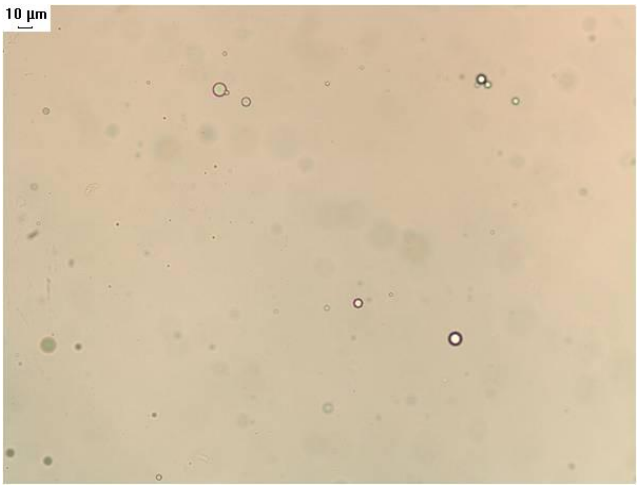

Figure 4.13. Ovalbumin plus silicone oil sample, after incubation, still contained oil droplets and some small protein like particles. There appeared to be some association of the protein with the oil droplets. 100X total magnification.

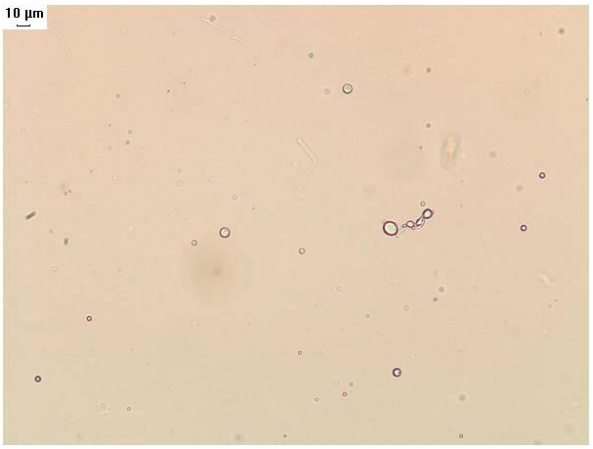

Figure 4.14. The Ovalbumin sample, after heating, contained a great deal of sheet like and fibrous aggregates as shown. 100X total magnification.

Figure 4.15. The Ovalbumin and silicone oil sample, after heating, showed a significant change in particle morphology. Some spherical particles resembling silicone oil droplets were seen, as well as many equant aggregates. 100X total magnification.

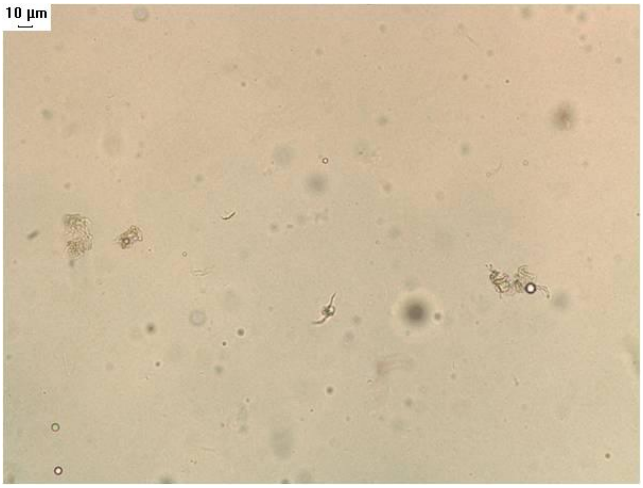

Figure 4.16. Representative aggregates found in the ovalbumin plus silicone oil samples after heating. The morphology of the aggregate was more equant and was associated with silicone oil droplets. 200X total magnification.

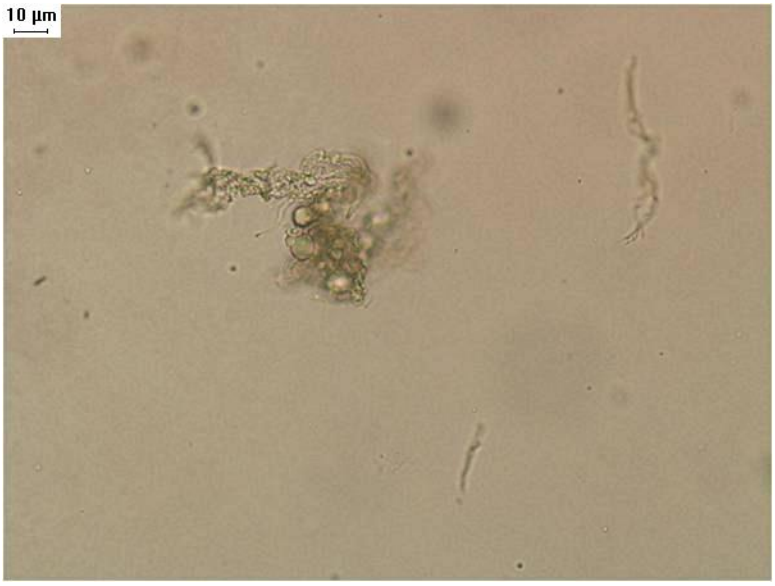

Figure 4.17. Representative aggregates found in the ovalbumin plus silicone oil sample after heating. This high magnification photo shows the protein aggregate associated with the silicone oil droplets. The spherical morphology and optical properties of the oil droplets were easily identified. 400X total magnification.

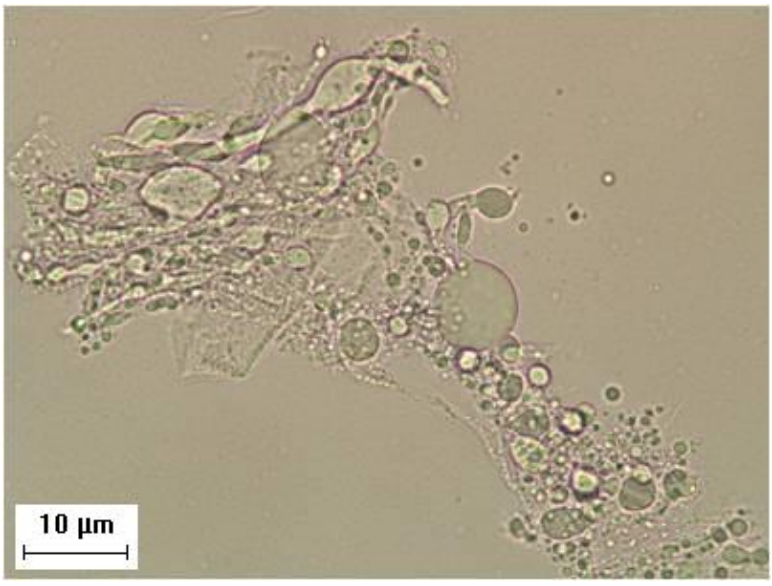

4.3.2.4 Fluorescence Microscopy

Based on the change in aggregate morphology observed with the presence of silicone oil, an additional study was conducted to further characterize these particles. Dyes have been used to enhance the contrast of protein particles, as discussed earlier in this report. Fluorescence microscopy was employed to aid in visualizing the protein aggregates formed in the presence of silicone oil droplets. Nile red dye was added to the various protein solutions immediately before viewing under the microscope (structure shown below).

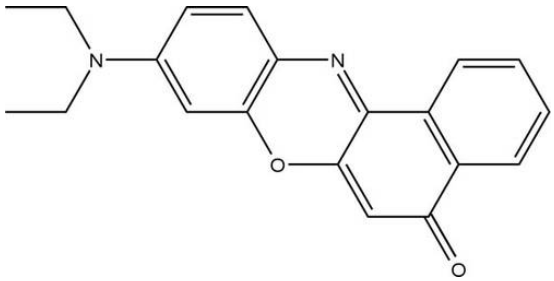

Nile Red
$C_{20}H_{18}N_2O_2$
MW: 318.369 g/mol

Structure 4.1

It was observed that the silicone oil emulsion sample provided minimal fluorescence when mixed with the dye (Figure 4.18), suggesting that the dye does not interact with the oil. This confirmed that a low background would be achieved when analyzing samples. In addition, dye was added to a solution containing ovalbumin and silicone oil droplets, and again there was very little dye associated with the droplets (photo not shown). Next, samples of ovalbumin and BSA, stressed through heating (as described previously), were

mixed with nile red and observed by microscopy (no oil added). Protein aggregates were seen in all samples, as shown in Figures 4.19 and 4.22. The aggregates were large and primarily sheet like and fibrous in morphology.

Next, the protein samples were heated in the presence of silicone oil and the nile red dye added to the samples. The protein aggregate morphologies were altered in the presence of the oil. Aggregates were smaller and more equant in shape. Figures 4.20-4.21 and 4.23-4.24 show representative aggregates observed with silicone oil present.

Figure 4.18. Silicone oil emulsion sample and nile red dye. Very little fluorescence intensity was observed. 100X total magnification.

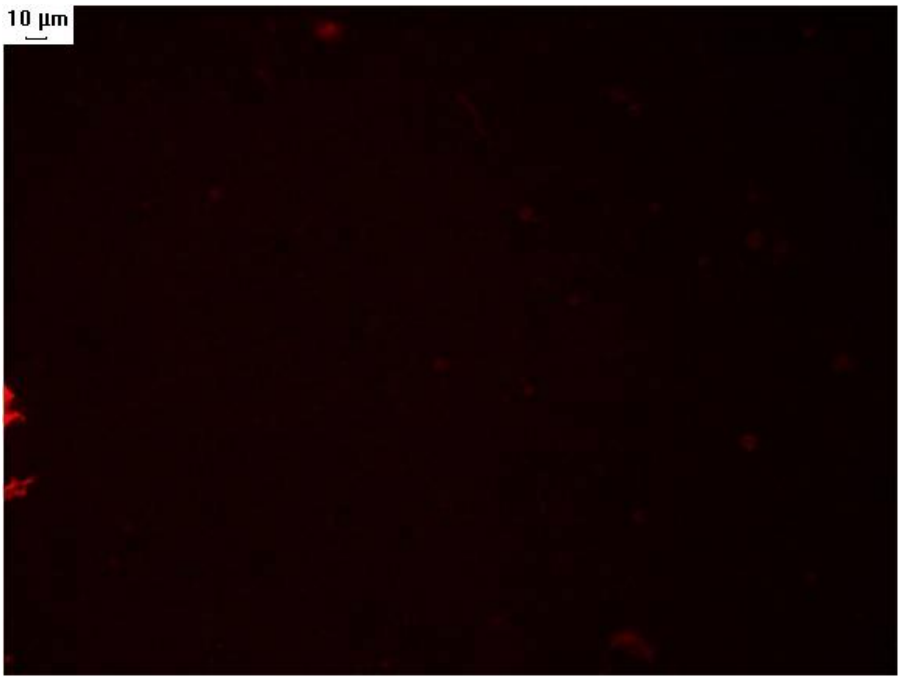

Figure 4.19. BSA, heated, mixed with nile red dye. Large sheet like aggregates were formed. A representative aggregate is shown, 100X total magnification.

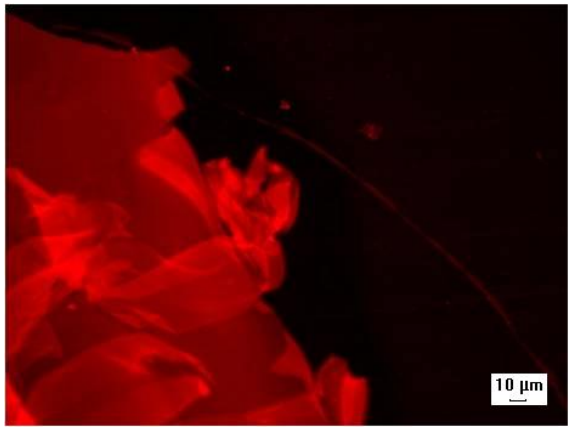

Figure 4.20 . BSA plus silicone oil sample, after heating. Much smaller and more equant particles as well as shorter fibers seen. 200X total magnification.

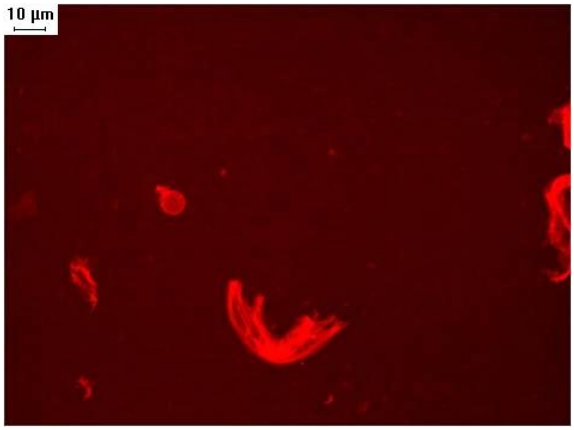

Figure 4.21. BSA plus silicone oil sample, after heating. 100X total magnification.

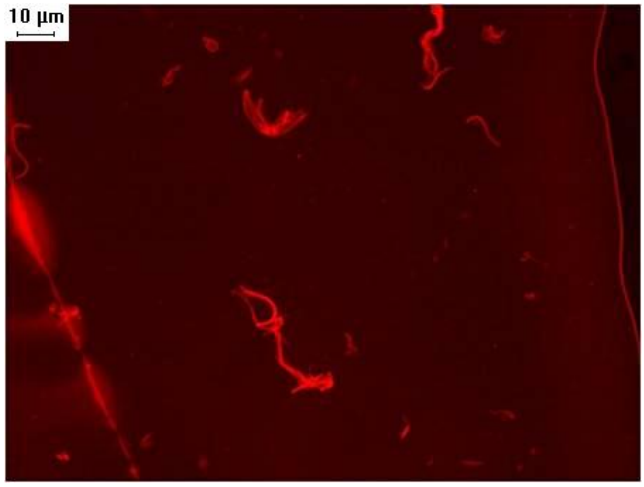

Figure 4.22. Ovalbumin, heated, mixed with nile red dye. Sheet like aggregates were observed, as shown. 200X total magnification.

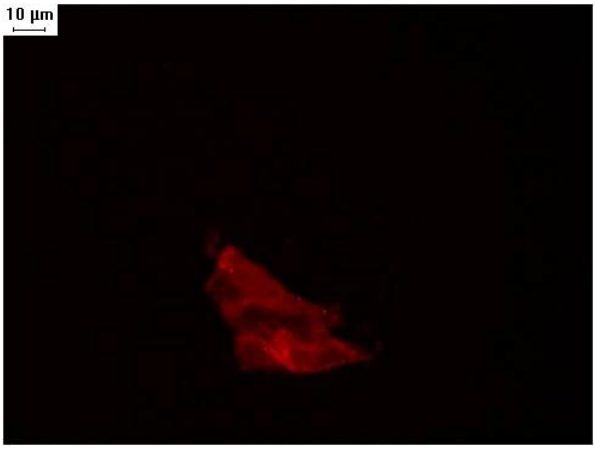

Figure 4.23. Ovalbumin plus silicone oil sample, after heating. 400X total magnification.

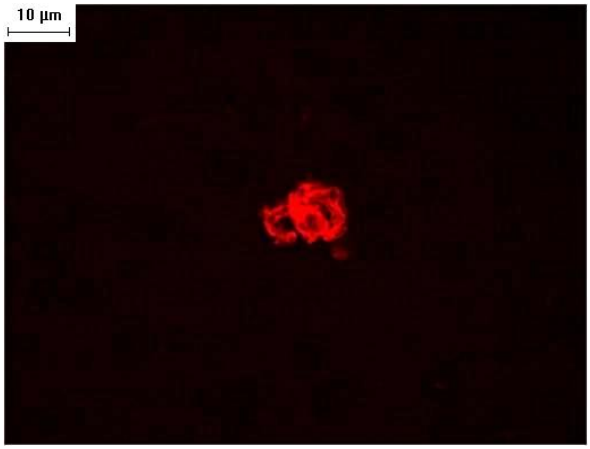

Figure 4.24. Ovalbumin plus silicone oil sample, after heating. 400X total magnification.

4.4 Discussion

After a period of incubation, the silicone oil emulsion sample had a decrease in larger particles. However, in the presence of protein, the larger oil droplets are still observed,

suggesting that they are being stabilized by the protein in solution. In the case of ovalbumin, the association of protein and silicone oil was readily observed by optical microscopy. DSC suggested that silicone oil does not affect the Tm of the proteins studied. It has been demonstrated previously, that silicone oil at 0.5%, had slight to no effect on the thermal unfolding temperature (Tm) of model proteins including BSA [37].

An objective of this study was to determine what techniques could be used to characterize particles in protein solutions, when silicone oil droplets are present. Optical microscopy can provide a quick and easy method for determining the morphology and abundance of particles in solution (with a lower limit of resolution around 1-2 μm). In addition, the study suggested that in the presence of silicone oil, protein aggregate morphology can be affected. If the protein associates with the silicone oil droplets, a smaller and more equant aggregate may form. This has implications in particle size and count analysis, especially if samples are being analyzed during drug product development and later introduced to a siliconized surface such as a pre-filled syringe. Also, protein has been observed coating silicone oil droplets (Figure 4.24). In this situation, the particles could not be differentiated from silicone oil droplets by techniques such as flow imaging. The ability to differentiate silicone oil particles from protein was a goal of this work. Although a visible dye can provide some contrast between a protein coated oil droplet and non-coated droplet, a fluorescent dye can greatly enhance this contrast. The fluorescent dye associated with the protein where minimal to no interaction took place with the oil. Particles were viewed using a fluorescent microscope. Image analysis can

be employed for further analysis including information on morphology and how protein might be associated with the oil.

4.5 Summary

The results of this study suggest that silicone oil droplets can interact with protein, especially when the protein solution is undergoing a stress (thermal, mechanical, etc.). Moreover, the ensuing particles can be quite different in morphology from the aggregates that would form without oil droplets present. It is assumed that as the protein unfolds and aggregates, hydrophobic areas become exposed. This increased hydrophobicity (exposure of hydrophobic protein groups) can lead to attraction of other hydrophobic surfaces such as the pendant methyl groups off the silicone backbone in silicone oil [38]. Silicone oil droplets are abundant in prefilled syringes and found in certain vial stoppers [39]. When assessing the stability of protein solutions upon stress conditions such as heat or agitation, the presence of oil droplets could interfere with accurate particle characterization assays. It has been suggested that dynamic flow imaging (such as the Brightwell MFI) may be used to electronically 'filter' equant particles during analysis. Our data indicate caution should be used because these equant particles may actually be complexes of silicone oil droplets and aggregated protein, resulting in gross undercounting of protein particles. Care must be taken to assess the composition of the particles detected, especially in systems such as prefilled syringe. This dye-based assay, utilizing Nile red, provides a tool to differentiate silicon oil droplets from both protein-coated silicone oil droplets and protein aggregates.

Chapter 5. Summary and Future Work

The studies described in this dissertation allow for determination of particle counts and characterization of particles found in protein drug products using a minimal amount of sample volume. All methods were developed with the goal of providing the most information on protein aggregates, using the least amount of sample. In addition, it has been demonstrated that silicone oil particles do not appear to induce protein aggregation for the proteins studied, but silicon oil did interact with proteins during aggregation by incorporating into the aggregates, as was observed by optical microscopy. Fluorescence microscopy studies suggest that protein can also coat the silicone oil droplets. This can affect the physical properties of the protein aggregate, including morphology, creating a more uniform, equant aggregate, which may be of concern with respect to immunogenicity. This interaction also makes differentiation between protein/oil droplets and neat silicone oil droplets difficult, highlighting the need for new methods.

Future work will include further optimization of the low volume light obscuration method, including additional validation studies to determine the effect of viscosity when analyzing higher concentration protein samples (> 100 mg/mL). This method can provide results that meet the USP criteria, while minimizing the amount of sample needed for analysis. By performing these additional validation/robustness studies, the method can be transferred to routine analysis labs (such as a QC lab) for stability and release testing.

Additional work will also continue in the development of imaging techniques using visible and fluorescent dyes. These techniques are ideally suited for the characterization of larger (visible) protein particles. The use of a dye to enhance the visual contrast of protein particles and a filter membrane could be used to develop orthogonal techniques to visual inspection testing. With the use of automated image analysis, determination of the amount of particles as well as morphological and compositional information could be obtained. Enhancing the visualization of protein particles could be very advantageous when performing formulation development studies, where visual inspection is performed on vials with small volumes of drug product. The ability to detect translucent fibrous protein particles under those conditions is limited. One study that is ongoing, is the use of fluorescent dyes to enhance visualization of protein in the presence of silicone oil particles. Studies to understand the coating of a protein on a silicone oil droplet is of great interest.

It is well accepted that the amount and size of particles in parenteral products is a critical quality attribute. In addition, it is highly recommended that the composition of these particles be understood to fully understand the quality of the product. The techniques introduced here can be used to aid in characterization of particulate matter, using minimal amounts of sample.

Chapter 6. References

1. www.biopharma.com/approvals_2009
2. Manning, M., Patel, K., Borchardt, R.T. Stability of Protein Pharmaceuticals. *Pharm Res*. **1989**, 6(11): 903-918.
3. Manning, M., Chou, D., Murphy, B.M., Payne, R.W., Katayama, D.S. Stability of Protein Pharmaceuticals: An Update. *Pharm Res*. **2010**, 27(4): 544-575.
4. Mahler, H., Friess, W., Grauschopf, U., Kiese, S. Protein Aggregation: Pathways, Induction Factors and Analysis. *J Pharm Sci* **2009**, 98(9): 2909-34.
5. Li, B., Gorman, E., Moore, K.D., Williams, T., Schowen, R.L., Topp, E.M., Borchardt, R.T. Effects of Acidic N+1 Residues on Asparagine Deamidation Rates in Solution and in the Solid State. *J Pharm Sci* **2005**, 94(3): 666-675.
6. Stratton, L.P., Kelly, M.R., Rowe, J., Shively, J.E., Smith, D.D., Carpenter, J.F., Manning, M.C. Controlling Deamidation Rates in Model Peptide: Effects of Temperature, Peptide Concentration, and Additives. *J Pharm Sci* **2001**, 90(12): 2141-48.
7. Robinson, N.E., Robinson, A.B. Deamidation of Human Proteins. *PNAS* **2001**, 98(22): 12409-12413.

8. Robinson, N.E., Robinson, A.B. Prediction of Protein Deamidation Rates from Primary and Three-dimensional Structure. PNAS **2001**, 98(8): 4367-72.

9. Cordoba, A.J. et al. Non-enzymatic hinge region fragmentation of antibodies in solution. *J Chromatogr* B **2005**, 818: 115-121.

10. Schellekens, H. How to predict and prevent the immunogenicity of therapeutic proteins. *Biotechnology Annual Rev*. **2008**, 14: 191-201.

11. Mire-Sluis, A., Cherney, B., Madsen, R., Polozova, A., Rosenber, A., Smith, H., Arora, T., Narhi, L. Analysis and Immunogenic Potential of Aggregates and Particles. A practical approach Part 1. *BioProc Intern*. **2011**, 9(10): 38-47.

12. Southall, S., Ketkar, A., Brisbane, C., Nesta, D. Particle Analysis as a formulation development Tool. *Am. Pharma. Rev.* **2011**, Sept/Oct.: 61-66.

13. Shabushnig JG, Melchore JA, Geiger M, Chrai S, Gerger ME. A proposed working standard for validation of particulate inspection in sterile solutions. Paper presented at: PDA Annual Meeting; **1994**, Philadelphia, PA.

14. Jiskoot, W., et al. Protein Instability and Immunogenicity: Roadblocks to Clinical Application of Injectable Protein Delivery Systems for Sustained Release. *J Pharm Sci*. **2012**, 101(3): 946-954.

15. Jones, L., Kaufmann, A., Middaugh, R. Silicone Oil Induced Aggregation of Proteins. *J Pharm Sci.* **2005**, 94(4): 918-927.

16. Strehl, R., et al. Discrimination Between Silicone Oil Droplets and Protein Aggregates in Biopharmaceuticals: An Novel Multiparametric Image Filter for

Sub-visible Particles in Microflow Imaging Analysis. *Pharm Res.* **2012**, 29:594-602.

17. Auge, K., et al. Demonstrating the Stability of Albinterferon Alfa-2b in the Presence of Silicone Oil. *J Pharm Sci.* **2011**, 100(12): 5100-5114.

18. Brown, L., Characterizing Biologics Using Dynamic Imaging Particle Analysis. *www.Biopharm International.com*. Aug 2, 2011.

19. USP, General Chapters: <788> Particulate Matter in Injections. USP 34-NF29

20. Carpenter, J.F., et al. Overlooking Subvisible Particles in Therapeutic Protein Products: Gaps That May Compromise Product Quality. *J Pharm Sci.* **2009,** 98(4): 1201-1205.

21. Narhi, L.O., Jiang, Y., Cao, S., Benedek, K., Shnek, D. A Critical Review of Analytical Methods for Subvisible and Visible Particles. *Current Pharm Biotech.* **2009,** 10:373-381.

22. Rosenberg, AS. Effects of Protein Aggregates: An Immunologic Perspective. *AAPS Journal*. **2006**, 8(3): E501-E507.

23. Singh, S.K., Impact of Product-Related Factors on Immunogenicity of Biotherapeutics. *J Pharm Sci*. **2011**, 100(2): 354-387.

24. Sharma, DK, King D, Moore, P, et al. Flow microscopy for particulate analysis in parenteral and pharmaceutical fluids. *Eur J Parenter Pharm Sci.* **2007**; 12(4): 97-101.

25. Wuchner, K. Analytical Development of MicroFlow Digital Imaging Method to Characterize Proteinaceous Particles. *IABS/FDA Conference*. Maryland, **2009**.

26. Huang, C, Sharma, D, Oma, P, Krishnamurthy, R. Quantitation of Protein Particles in Parenteral Solutions Using Micro-Flow Imaging. *J Pharm Sci.* **2009**, 98(9): 3058-3071.

27. Sharma, D, Oma, P, Pollo, M, Sukumar, M. Quantification and Characterization of Subvisible Proteinaceous Particles in Opalescent mAb Formulations Using Micro-Flow Imaging. *J Pharm Sci.* **2010**, 99(6): 2628-2642.

28. Scherer, G. Issues and challenges of sub-visible particulate analysis in protein solutions. Poster: AAPS-BITC Workshop: Sub-visible particulate characterization. Washington, **2009**.

29. Krishnamurthy, R. Comparison between light obscuration and imaging analyses for sub-visible particle counting. *ABS-FDA Protein Particles Conference*. Maryland, **2009**.

30. Feigl. *Spot Tests in Organic Analysis;* 7th ed. Elsevier Scientific Publishing Co.: New York, 1975 (p 370-372).

31. Kingsley, G.R.; Getchell, G. The determination of microgram quantities of protein in biological fluids. The estimation of plasma and serum protein in spinal fluid. *J. Biol. Chem*. **1957**, 225: 545-556.

32. Zaia, D.; Marques, F; Zaia, C. Spectrophotometric determination of total proteins in blood plasma: a comparative study among dye-binding methods. Brazilian Arch. Biol. Tech. **2005**, 48 (3): 385-388.

33. S. Ketkar, A., Brisbane, C., Nesta, D. Particle Analysis as a Formulation Development Tool. *American Pharma Review*. Sept/Oct 2011.

34. K.B., et al. Demonstrating the Stability of Albinterferon Alfa-2b in the Presence of Silicone Oil. *J. Pharm Sci*. **2011**, 100(12): 5100-5114.

35. Ludwig, D.B., Carpenter, J.F., Hamel, J., Randolph, T.W. Protein Adsorption and Excipient Effects on Kinetic Stability of Silicone Oil Emulsions. *J Pharm Sci*. **2010**, 99(4): 1721-1733.

36. Haskard, C., Li-Chan, E. Hydrophobicity of Bovine Serum Albumin and Ovalbumin Determined Using Uncharged (PRODAN) and Anionic (ANS-) Fluorescent Probes. *J Agric Food Chem*. **1998**, 46: 2671-2677.

37. Jones, L.S., Kauffmann, A., Middaugh, R.C. Silicone Oil Induced Aggregation of Proteins. *J. Pharm Sci.* **2005**, 94(4): 918-927.

38. Bartzoka, V., Chan, G., Brook, M. Protein-Silicone Synergism at Liquid/Liquid Interfaces. *Langmuir*. **2000**, 16: 4589-4593.

39. Harrison, B., Rios, M. Developments in Prefilled Syringes. *Pharma Techn*. **2007**, 31(3).